



# Contents

<b>1</b>	<b>Introduction to <math>\gamma</math>-Ray Astronomy</b>	<b>3</b>
1.1	Cosmic-ray physics	4
1.2	Acceleration mechanisms	5
1.2.1	Diffusive Shock Acceleration	5
1.3	Production of $\gamma$ -rays	7
1.3.1	Bremsstrahlung	8
1.3.2	Synchrotron emission	8
1.3.3	Curvature radiation	10
1.3.4	Inverse Compton scattering	10
1.3.5	Matter-Antimatter annihilation	11
1.3.6	Radioactive nuclei	11
1.3.7	Hadronic collisions	11
1.4	$\gamma$ -ray Absorption mechanisms	12
1.4.1	Interaction with electrons	12
1.4.2	Pair production processes	12
1.4.3	The Extragalactic Background Light	12
1.5	Dark Matter and $\gamma$ -rays: WIMP annihilation	13
1.6	$\gamma$ -ray sources	17
1.6.1	Galactic sources	17
1.6.2	Extragalactic sources	22
1.6.3	Potential Dark Matter annihilation emission sources	26





# 1. Introduction to $\gamma$ -Ray Astronomy

During many centuries humanity has looked towards the skies and wondered about the mysteries of the universe. At first, with the naked eye, our ancestors measured the movements of astronomical objects and used them as calendars and guidance. Since the invention of the optical telescope by Galileo in 1609 AD we can say modern Astronomy was born. However, we were looking only to a small part of the universe, being only able to study the stars through the visible light they were emitting. Like an incomplete symphony where we can only listen to the melody of one instrument, our knowledge of the physics of the cosmos was incomplete and purely limited to the thermal emission of stars. It wasn't until the first half of the XX century that we could start talking about the so called multi-wavelength astronomy with the first infra-red, radio, ultraviolet and X-ray observations. The last part of the electromagnetic spectrum,  $\gamma$ -rays were first detected in the 1960s. The emission of this high energy radiation (above 100 keV) couldn't be explained anymore with thermal processes, they should come from the new *non-thermal* universe. In 1989 the first detection of Very High Energy (VHE) gamma-rays was possible thanks to the Whipple collaboration, the first Imaging Atmospheric Cherenkov Telescope, which for the first time detected  $\gamma$ -ray emission from the Crab nebula, a Pulsar Wind Nebula Pulsar Wind Nebula (PWN).

Along with the multiwavelength astronomy, other messengers from the sky that evidenced the existence of non-thermal processes were discovered: In 1912 the Austrian physicist Victor Hess discovered that the puzzling source of high levels of ionizing radiation in the atmosphere were actually charged particles coming from space. These particles were later named *cosmic rays* by Millikan, and as will be explained later, their origin was thought to be closely related to the origin of VHE  $\gamma$ -rays, because  $\gamma$ -rays are produced in relativistic particles interactions.

Because of the close relation of particle physics (cosmic-rays) and astrophysics ( $\gamma$ -rays) the new field that Hess and Whipple opened was called Astroparticle Physics, which together with the multi-messenger astronomy, is a fascinating new window towards the completion of the cosmic symphony that is the Universe.

This chapter will be an overview of the basic concepts of cosmic-ray and  $\gamma$ -ray physics, their production, acceleration and absorption, and their known sources of emission in the

universe.

## 1.1 Cosmic-ray physics

Cosmic Rays (CRs) are relativistic charged particles arriving to the atmosphere from the outer space. The truth of their origin and the mechanisms that produce their acceleration to reach such high energies is still unknown. However, it is well believed that they are accelerated in very violent events in the universe, such as supernova explosions.

As they are charged particles, they suffer from the effects of the magnetic fields (both interstellar and Earth magnetic fields) which divert their trajectories and make very difficult to trace back their original direction. Since  $\gamma$ -rays, which are neutral, can be produced by several particle interaction processes, such as Inverse Compton scattering or decay of neutral pions, among others (see section 1.3), the detection of  $\gamma$ -rays is a way to understand how and where do CRs interact with the medium.

The composition of CRs arriving to the Earth is mainly protons (86%), alpha particles (11%), other heavy nuclei (1%) and electrons (2%). We can distinguish between two types of cosmic-rays: If they reach the Earth unaltered from their sources, they are known as *primary CRs*, while if they come as the product of inelastic collisions in the Interstellar Medium (ISM), they are called *secondary CRs*.

The spectrum of CRs is shown in figure 1.1. For the most part of the spectrum it can be described as a Power Law:

$$N(E)dE \propto E^{-\gamma} \quad (1.1)$$

where the spectral index  $\gamma$  is different in the three distinguishable regions of the spectrum:

- Up to the *knee* (below  $10^6$  GeV): CRs in this energy range are produced by solar wind. They follow a simple power law with spectral index  $\gamma \sim 2.7$ .
- From the *knee* to the *second knee* (at  $10^8$  GeV) the spectral index becomes  $\sim 3.1$ .
- Between the *second knee* (at  $10^8$  GeV) and the *ankle* the spectral index is  $\sim 3.3$ . CRs between the *knee* and the *ankle* are considered to be accelerated within the galaxy, being Supernova Remnants (SNRs) the best candidates to be CR accelerators.
- Energies above the *ankle* ( $\sim 10^9$  GeV): In this region, CRs coming from extragalactic sources are predominant. At such high energies, particles are no more confined by galactic magnetic fields so they travel with their trajectories unperturbed, allowing to do estimations of their direction. These kind of very energetic CRs can be produced in Active Galaxy Nuclei (AGN), Gamma Ray Bursts (GRBs), radio galaxy lobes and intra-cluster medium in galaxy clusters. In this region the spectrum hardens to  $\gamma \sim 2.7$ .
- At energies above  $\sim 4 - 5 \cdot 10^{10}$  GeV a strong suppression is observed, named the GZK cutoff, which can be interpreted as a theoretical upper limit on the energy carried by CR from distant sources.

From the regions described above is possible to differentiate two possible CR origins: galactic CR and extragalactic CR. Below the ankle, CRs are produced in galactic accelerators (SNRs) and this energy can be considered a limit on the acceleration that is possible to gain from these kind of objects. CRs with higher energies come from extragalactic sources and so,

their higher acceleration must come from different phenomena, more violent and energetic (AGN, GRBs, etc.). The transition in the spectrum can be explained by the effect of the galactic magnetic field in the trajectories of the cosmic rays. The Larmor radius (eq. 1.2) defines the curved trajectory of charged particles moving perpendicular to a magnetic field. For energies over the knee it starts to become larger than galactic scales, hence extragalactic CRs propagate linearly and unaffected by the galactic magnetic field, while galactic (less energetic) CRs propagate diffusively through the ISM.

About the exact chemical composition of primary CR, it has been noticed that their abundances are similar to the ones of Solar System, but with some essential differences regarding Li, Be and B. The abundances of these elements are small in stars because they are rapidly consumed by nuclear reactions, but they are present in CRs due to *spallation* of carbon and oxygen nuclei [66].

$$r_g = \frac{cp_{bot}}{ZeB} \approx 100pc \frac{3\mu G}{B} \frac{E}{Z \times 10^{18}eV} \quad (1.2)$$

## 1.2 Acceleration mechanisms

The mechanisms that accelerate CRs to the huge energies observed, that can reach up to  $10^{20}$  eV are still a topic of debate and research in the high energy astrophysics field. Several particle acceleration mechanisms are proposed to explain the CR spectra. To do so, we need a mechanism capable not only to achieve the highest energies measured for CR, but also the spectral shape of a power law with an index  $\sim 2.7$ , and their abundances. In [49] an extensive discussion on several possible acceleration mechanisms can be found, mainly distinguishing between two types of acceleration:

- *Statistical acceleration*: In this case the acceleration takes place gradually when particles encounter different regions of moving magnetic fields. This process can reach a power law spectrum of index  $\sim 2$ , but is slow and energy losses are difficult to account at high energies.
- *Direct acceleration*: Strong electric fields like the ones generated during magnetic field reconnection in magnetospheres can directly accelerate particles. However, the mediums where this may occur are very dense, leading to energy losses.

Among all the possibilities each of them with their caveats and benefits, it is in general accepted that galactic CRs are accelerated in SNRs (for a more detailed discussion on these objects, see section 1.6.1). This statement is supported by the fact that the energy density of CRs is compatible with the power supplied by a Supernova (SN) according to the SN rate and CRs lifetime in the galaxy.

### 1.2.1 Diffusive Shock Acceleration

The most popular acceleration mechanism to explain acceleration in SNRs is known as Diffusive Shock Acceleration (DSA) or *First Order Fermi acceleration*. This mechanism revisits the original idea formulated by Fermi in 1949 [37], of particles colliding with

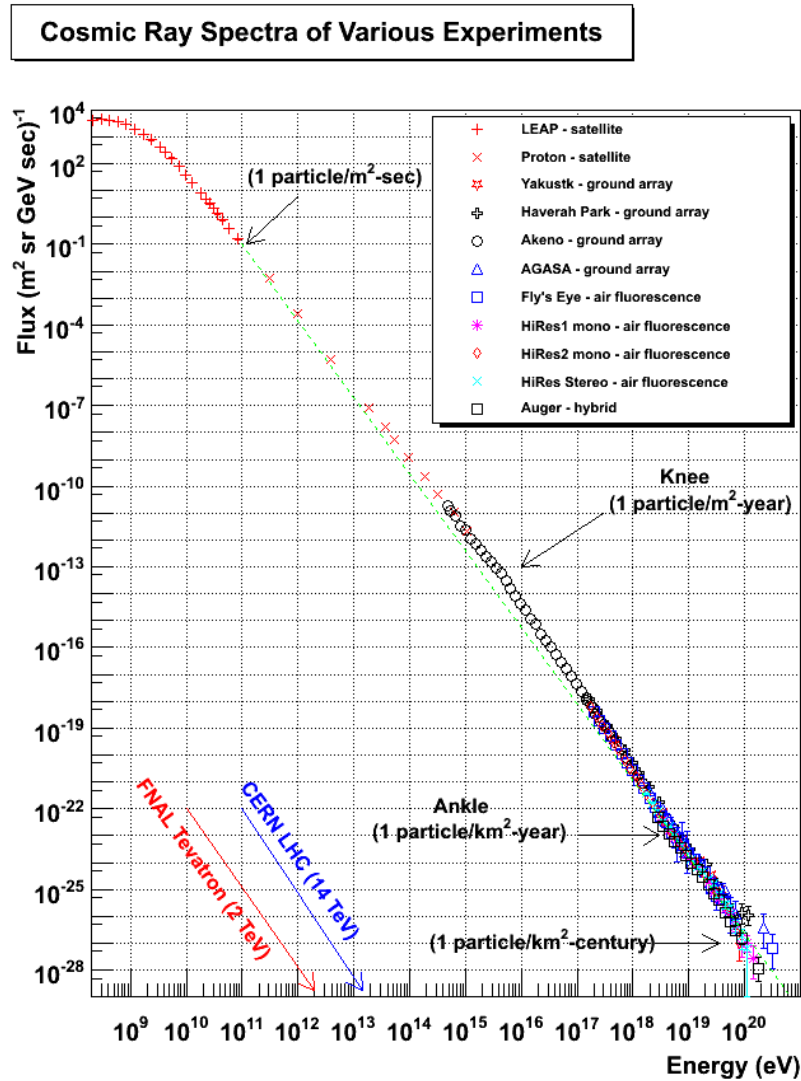


Figure 1.1: Cosmic ray spectrum from [47]. Green line shows the fit to a power law with spectral index 2.7.

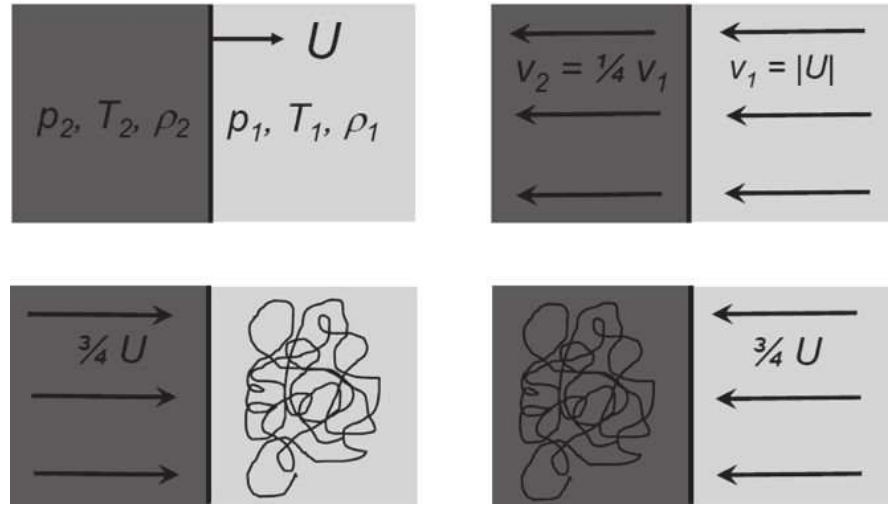


Figure 1.2: Scheme of the *Diffuse shock acceleration* from [58]. *Upper left.* Observer frame: A diffusive shock is propagating at velocity  $U$ . *Upper right.* Frame where the shock front is at rest. The velocities of the gas in both sides of the front, assuming it is fully ionized, have a ratio of 4. *Lower left.* Frame of reference where the upstream gas is at rest, the distribution of velocities of the high energy particles is isotropic. *Lower right* Same case as previous, but in the reference frame of the downstream gas.

randomly moving "magnetic mirrors" in the ISM, but happening in the presence of strong supersonic shock waves propagating through a diffuse medium, like the ones produced after a SN explosion (see figure 1.2). A flux of relativistic particles is assumed to exist in both sides of the shock, which are moving much faster than the latter. Each time a particle crosses to one side or the other, their velocity becomes isotropic in the frame of reference of the moving fluid. Since on every crossing the particle encounters gas moving towards it at a velocity proportional to the shock velocity ( $U$ ), which for a fully ionized plasma is  $\sim 3/4U$  it will receive a boost in energy of the order  $\sim U/c$ . That is why this process is called *first order* in counterpart to the classical *second order Fermi acceleration* where the energy gain in each collision is proportional to  $\sim (U/c)^2$ . While this mechanism easily predicts a power law spectrum, the index is 2 instead of 2.7. Moreover, it exists an upper limit on the maximum energy that a particle can gain through DSA which is set to  $\sim 10^{14}$  eV. This process has become a key part of CR physics since its discovery in the 70's, but it is still not enough to explain the full CR spectrum.

### 1.3 Production of $\gamma$ -rays

$\gamma$ -rays are the most energetic radiation in the electromagnetic spectrum. The range of energies goes from 100 KeV to hundreds of TeV.

When we talk about radiation production, we can distinguish between two main mechanisms which involve very different physical phenomena: Thermal and non-thermal processes. The low energy radiation (up to X-rays) emitted by stars or interstellar dust is produced by thermal processes following a black body spectrum. The intensity of the radiation only depends on the temperature of the object by the Planck formula. To produce radiation as

energetic as  $\gamma$ -rays we would need a temperature of the order of  $10^{10}$  K, which is something that was only reachable in the Big Bang conditions. Therefore to understand the production of  $\gamma$ -rays we must study the so called *non-thermal universe*, where radiation is produced by relativistic particles moving in electromagnetic fields. Here we can sense the close relationship between CR and  $\gamma$ -ray astronomy.

In general, we can say that  $\gamma$ -rays will be produced in two kinds of scenarios: leptonic emission (produced mainly by electrons) and hadronic emission (produced mainly by protons). Which one of those is dominant in astrophysical particle accelerators is still unknown, and it is an open discussion issue on the puzzle of CR origin. In this section a brief summary on the different  $\gamma$ -ray production mechanisms (see figure 1.3) is given.

### 1.3.1 Bremsstrahlung

From the German 'braking radiation', the bremsstrahlung process occurs when a charged particle is moving in the electric field produced by an atomic nucleus. While their trajectory is deflected, the particle emits electromagnetic radiation with amplitude proportional to the acceleration suffered (which is actually a deceleration). The efficiency of this process is proportional to the ratio between the particle mass and charge, that is why generally, it is considered to be produced mainly by electrons which have a lower mass than other charged particles such as protons. The emitted photons after a charged particle suffers several interactions passing through a medium, will have a continuum spectrum following the same power law as the particle. Bremsstrahlung is the dominant process in the production of galactic diffuse  $\gamma$ -ray emission up to  $\sim 100\text{MeV}$ . It takes place in gaseous nebulae that contain ionized gas and in the intracluster medium of galaxy clusters.

### 1.3.2 Synchrotron emission

Synchrotron emission is produced when a charged relativistic particle is moving in a magnetic field. The particle will follow an spiral path, with constant velocity along the field lines, while being accelerated towards the center of its orbit. It will suffer an energy loss in the form of synchrotron radiation, with a total loss rate:

$$-\left(\frac{dE}{dt}\right) = \frac{e^4 B^2}{6\pi\epsilon_0 c m_e^2} \frac{v^2}{c^2} \gamma^2 \sin^2\alpha \quad (1.3)$$

Where e is the charge of the particle, B is the magnetic field,  $\alpha$  is the pitch angle of the spiral path of the particle and  $\gamma$  is the Lorentz factor of the electron. Following 1.3, note that again the power emitted will be inversely proportional to the mass of the particle hence this process is dominated by electrons (or positrons), being very inefficient for protons. The spectrum emitted by mono-energetic electrons is a continuum with maximum energy:

$$E_\gamma = 5 \times 10^{-9} B \left[ \frac{E_e}{m_e c} \right]^2 (\text{eV}) \quad (1.4)$$

Where B is the magnetic field component perpendicular to the particle trajectory, and  $E_e$  is their energy.

Synchrotron radiation of ultra-relativistic particles is the most important contribution to the non-thermal universe. It is responsible of the emission in SNRs and of the non-thermal

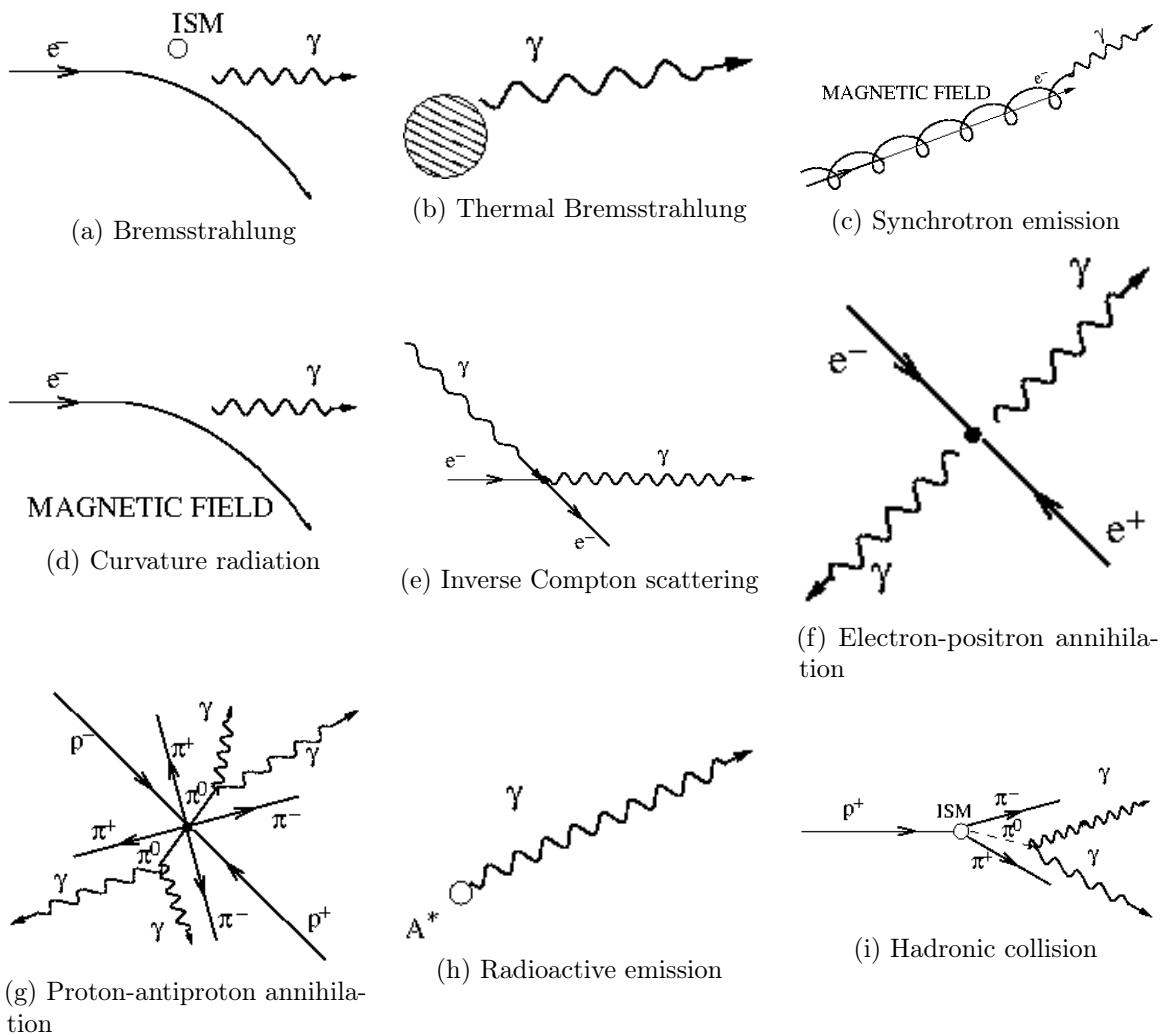


Figure 1.3: Diagrams of the different  $\gamma$ -ray production processes. Figures extracted from [65].

optical continuum from the Crab nebula. According to 1.4, it will require too high values of  $B$  and  $E_e$  to produce High Energy (HE)  $\gamma$ -rays (unless it is produced by Ultra High Energy Cosmic Rays (UHECRs)), but it can produce seed photons for Inverse Compton scattering (section 1.3.4), which will acquire much higher energies.

### 1.3.3 Curvature radiation

In presence of very strong magnetic fields, of the order of  $10^{11}$ - $10^{13}$  G, an electron will be forced to follow a trajectory parallel to the magnetic field lines. Since they are curved, with a curvature radius  $\rho_s$ , the particle will emit *curvature radiation* in the direction of movement, with an energy loss of the form [73]:

$$P = \frac{2}{3} \frac{e^2}{c^3} \gamma^4 \left( \frac{c^2}{\rho_c} \right)^2 \quad (1.5)$$

Charged particles in the surroundings of pulsars are able to produce curvature radiation due to the extremely high magnetic fields close to their surfaces, being able to produce HE  $\gamma$ -rays up to GeV if the relativistic particle has TeV energies.

### 1.3.4 Inverse Compton scattering

Inverse Compton (ic) scattering is the inelastic interaction between a relativistic electron and a photon. The result is the transfer of part of the energy of the particle to the photon. It is a fundamental process for HE /*gamma*-ray emitters since it can produce photons with energies from  $\sim 1\text{MeV}$  to  $\sim 1\text{TeV}$ . We can differentiate between two regimes depending on the initial energy of the photon, which will be seen Doppler shifted in the frame of the relativistic electron with energy  $\gamma h\nu$ :

- *Thomson regime*: If  $\gamma h\nu \ll m_e c$ , electron recoil can be neglected and the average energy of the photon after the scattering follows:

$$\langle E_\gamma \rangle \simeq \frac{4}{3} \langle \epsilon \rangle \gamma^2 \quad (1.6)$$

Where  $\epsilon$  is the energy of the photon before the scattering.

- *Klein-Nishina regime*: When  $\gamma h\nu \gg m_e c$ , electron recoil is significant and in this case the average energy of the photon after the interaction is:

$$\langle E_\gamma \rangle \simeq \frac{1}{2} \langle E_e \rangle \quad (1.7)$$

Where  $E_e$  is the energy of the electron.

In the transition between the two regimes, electrons will lose most of their energy in just one interaction rather than cooling progressively.

Photons from the Cosmic Microwave Background (CMB) are typical targets for ic scattering, together with synchrotron photons or photons thermally emitted by astrophysical sources. This mechanism is very important in VHE  $\gamma$ -ray emitters, like in the jets of AGN

and TeV blazars. The spectrum of the photons emitted by this process will follow a power law related to that of the population of relativistic electrons in the medium:

$$\frac{dN_\gamma}{dE} \propto E^{-\frac{(\alpha+1)}{2}} \quad (1.8)$$

### 1.3.5 Matter-Antimatter annihilation

Matter-antimatter pair annihilation processes can produce  $\gamma$ -rays. The most common case is electron-positron annihilation ( $e^-e^+ \rightarrow 2\gamma$ ). If the two particles are at rest, they produce  $\gamma$ -rays with energy equal to their masses (0.511 MeV). In the case the particles are moving, they can produce positronium, which has a high chance of decaying in 3  $\gamma$ -rays with an energy continuum peaking at 0.511 MeV. Proton-antiproton annihilation can also produce  $\gamma$ -rays indirectly by the production of neutral pions  $\pi^0$  which decay into  $\gamma$ -rays later on. However, this is a very uncommon process because the creation of anti-protons by proton interaction with matter is very unlikely.

### 1.3.6 Radioactive nuclei

Radioactive nuclei can also produce low energy  $\gamma$ -rays when decaying after being excited by the interaction of a proton with elements in the surrounding medium.

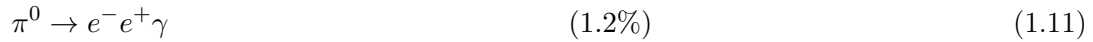
### 1.3.7 Hadronic collisions

While most of the processes described above were dominated by electron interactions (leptonic scenario), we now focus on the processes that constitute the hadronic contribution to the production of  $\gamma$ -rays, which are believed to be the dominant  $\gamma$ -ray production processes in SNRs and AGN.

Protons accelerated to relativistic energies in extreme environments, such as strong magnetic fields or jets can collide with other hadrons producing mesons, kaons and hyperons. The most common interaction is the proton-proton collision to produce pions ( $\pi$  mesons):



Neutral pions  $\pi^0$  decay into  $\gamma$ -rays within a short lifetime  $\tau = 8.6 \cdot 10^{-17}$ s through the channels:



With a threshold energy of the proton for this process:

$$E_p = 2m_{\pi^0}c^2 \left(1 + \frac{m_{\pi^0}}{4m_p}\right) \simeq 280\text{MeV} \quad (1.12)$$

Then the energy of the photons emitted by the  $\pi^0$  peaks at  $E_\gamma = m_{\pi^0}c^2/2 \simeq 67.5$  MeV, but in the laboratory frame of reference this energy depends on the energy of the  $\pi^0$  and the

angle of the proton trajectory with respect to the  $\pi^0$  allowing the emitted  $\gamma$ -rays to reach very high energies.

While the decay of charged mesons is not important for the production of  $\gamma$ -rays, they can decay into neutrinos  $\nu_{e,\mu}$  with a spectrum similar to that of the photons. Finding a correlation between *gamma*-ray emission and astrophysical neutrinos from a certain source would be an unequivocal way to differentiate between leptonic and hadronic emission. Their spectrum shape and the lack of correlation with X-rays could be other ways to distinguish hadronic and leptonic emission.

## 1.4 $\gamma$ -ray Absorption mechanisms

Although they are very energetic,  $\gamma$ -rays can interact with matter while they are traveling through the universe from their source to the Earth. Unlike low energy light, they are not deflected by the surface of materials, but they can interact electromagnetically with the electrons within. In general,  $\gamma$ -rays rarely interact with matter due to the low density of the universe but they can interact with lower energy photons that widely populate the ISM, mainly formed by two types of radiation: the CMB and the Extragalactic Background Light (EBL), which involves all the light emitted by stars during the history of the universe and the re-processing of this light by dust and gas. Absorption of high energy photons will affect to the spectrum of  $\gamma$ -rays measured from Earth so characterizing the different absorption mechanisms is very important HE Astrophysics.

### 1.4.1 Interaction with electrons

$\gamma$ -rays of energies below 100keV can produce photoelectric effect in the surface of materials, removing electrons from atoms and so reducing the energy of the incident  $\gamma$ -ray. In a similar way, electrons can be hit by  $\gamma$ -rays in the range from 0.1 MeV to a few MeV, and gain a fraction of the photon's kinetic energy [74].

### 1.4.2 Pair production processes

The most common absorption mechanism for HE and VHE radiation is the production of a pair  $e^-e^+$  after the interaction of two photons.

A photon passing close to a charged particle can produce a pair  $e^-e^+$  when interacting with a virtual photon of the particle electric field in the so called *classical pair production*.  $\gamma$ -rays absorbed in the atmosphere suffer this phenomenon developing Extended Air Showers (EAS) which are key for ground based  $\gamma$ -ray detectors.

When a  $\gamma$ -ray interact with a real photon in the medium, they can produce a pair  $e^-e^+$  if the total energy of the two photons is larger than  $2m_ec^2$ . The absorption of  $\gamma$ -rays through this process while interacting with the EBL is specially relevant for distant (extragalactic) sources, since EBL absorption depends on the redshift.

### 1.4.3 The Extragalactic Background Light

The EBL is a fundamental constituent of the universe that permeates it uniformly. Direct measuring the EBL is a very difficult task, mainly because of the foreground light from the Solar System. Several direct measures have been done from the far infrared to the optical, but many discrepancies and uncertainties still remain [35]. Phenomenological approaches try

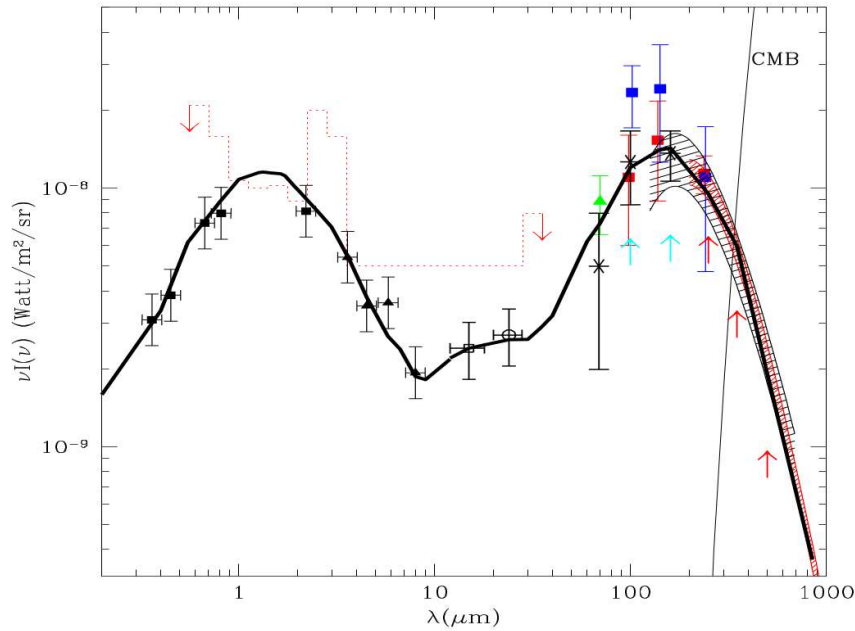


Figure 1.4: Best fit model prediction of the EBL energy density from [38] (thick black line).

to predict an EBL model based on galaxy formation and evolution during the history of the universe. Besides the different proposed models, it is accepted that their energy density is characterized by two peaks, as seen in figure 1.4. The first peak, found at  $\sim 1\mu\text{m}$  is known as the stellar component, being the product of the light of stars throughout the history of the universe. The second peak at  $\sim 100\mu\text{m}$  is known as the dust component, being the light re-emitted by cosmic dust.

The attenuation produced by the EBL to the spectrum of a  $\gamma$ -ray source at the energy  $E$  follows the form:

$$F = F_0(E) e^{\tau(E,z)} \quad (1.13)$$

Where  $F$  is the observed flux and  $F_0$  the intrinsic spectrum of the  $\gamma$ -ray source,  $\tau$  is an optical depth which depends on the energy and the redshift  $z$ . As a consequence of this dependence, for each energy there is a distance (redshift) at which the universe is optically thick to  $\gamma$ -rays, achieved when the optical depth is equal to 1. The spectrum of a  $\gamma$ -ray source will suffer a cutoff at the energy that reaches the threshold optical depth, which as it is shown in figure 1.5 decreases rapidly with redshift.

Observations of distant sources in the VHE range is very important to set constraints and characterize the EBL in an indirect way, to complement the direct measurements.

## 1.5 Dark Matter and $\gamma$ -rays: WIMP annihilation

The nature of Dark Matter (DM) is one of the most important open questions in modern physics. There are many probes that suggest that the universe is composed of something

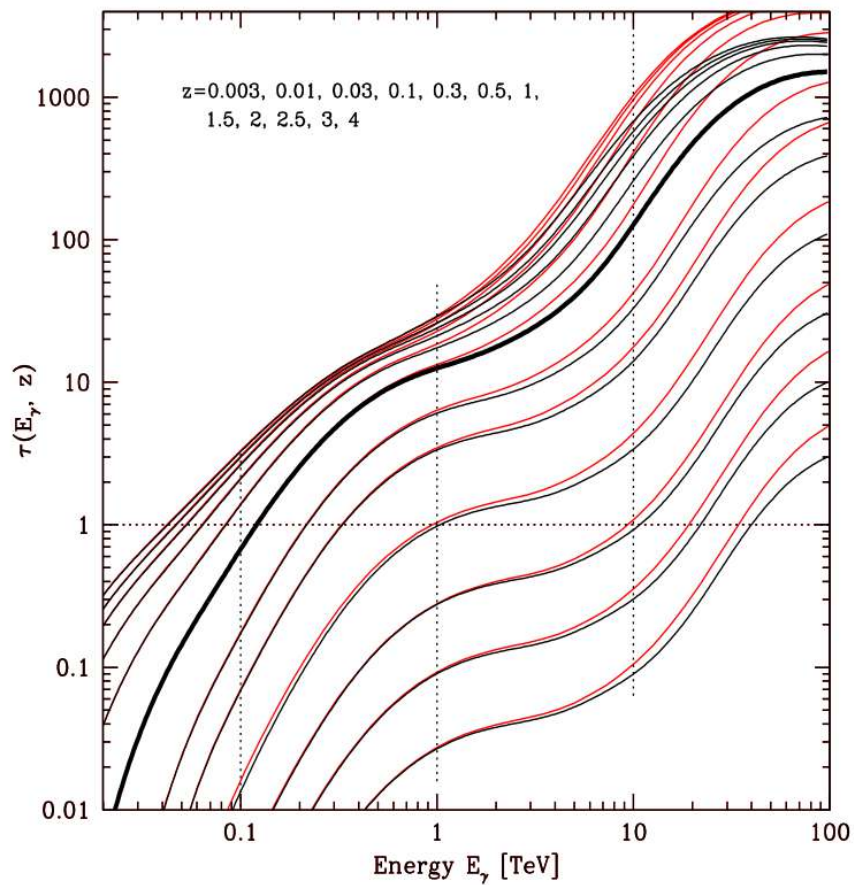


Figure 1.5: Optical depth by photon-photon collision as a function of energy for different redshift values, from [38].

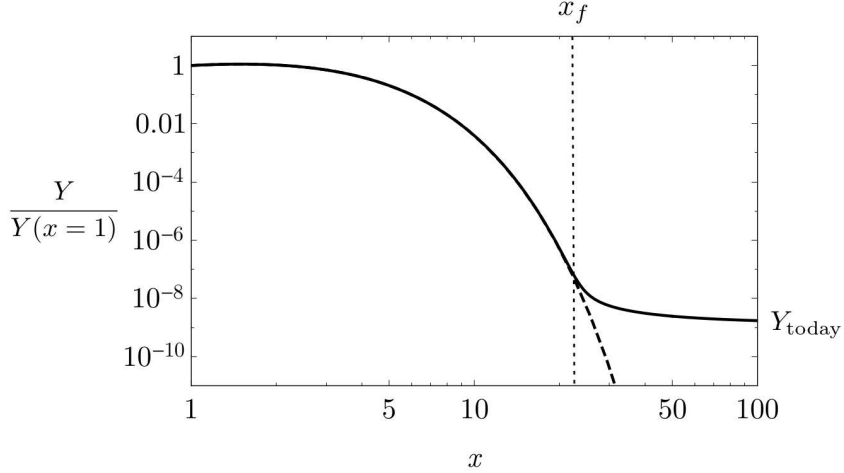


Figure 1.6: Evolution of Cold Dark Matter number density with time variable  $x$ ,  $x_f$  is the time of *freeze-out*, from [57].

more than the visible luminous matter: From the Fritz Zwicky measurements on the velocity dispersion in the Coma galaxy cluster [23] and the rotation curves of high-luminosity spiral galaxies obtained by Vera Rubin [72], to the much more modern measurements of the CMB by Planck [69] or observations regarding primordial Nucleosynthesis [63], all of them point to the existence of a non-baryonic type of matter which only interacts gravitationally with Standard Model (SM) particles. Many theories have been developed trying to solve the mystery of DM , and  $\gamma$ -ray astronomy has an important role in one of the most popular DM candidate theories. Thanks to cosmological simulations and cosmological probes such as Wilkinson Microwave Anisotropy Probe (WMAP) we know that DM must be non-relativistic (Cold Dark Matter (CDM)) that decoupled from the thermal equilibrium in the early universe. With these assumptions, we can derive the number density evolution of DM particles today from the Boltzmann equation, getting:

$$\frac{dY}{dx} = -\frac{xs\langle\sigma v\rangle}{H(m)}(Y^2 - Y_{eq}^2) \quad (1.14)$$

Where  $m$  is the mass of the DM particle,  $x$  is the scaled time variable  $x = m/T$  being  $T$  the temperature of the photon bath,  $s$  is the total entropy density of the universe and  $Y$  is the number density of DM reescaled to  $s$  ( $Y = n/s$ ) to account for the expansion of the universe. While the annihilation rate of the particles is higher than the expansion rate of the universe ( $\Gamma \gg H$ ), the number density  $Y$  remains close to  $Y_{eq}$ . After the moment of *freeze-out*, that is the moment when the particles can no longer find each other fast enough to interact (time  $\gg x_f$  where  $\Gamma \ll H$ ), the number density will remain almost constant as shown in figure 1.6.

Following the approach of [57], after freeze-out, the evolution of DM abundance can be written as:

$$\frac{dY}{dx} \approx -\frac{\lambda}{x^{n+2}}, \text{ where } \lambda = \frac{\langle\sigma v\rangle_0 s_0}{H(m)} \quad (1.15)$$

To define  $\lambda$  the dependency of the cross section and entropy with  $x$  was pulled out through the change of variables:  $\langle \sigma v \rangle = \langle \sigma v \rangle_0 x^{-n}$  and  $s = s_0 x^{-3}$ . Taking  $n=0$ , the DM abundance today would be  $\simeq \frac{x_f}{\lambda}$ . There is no particle in the DM that could retrieve the fraction of critical density  $\rho_{cr}$  contributed by DM measured today, but if we consider a weak interacting particle in the weak mass regime ( $m_\chi \sim 100$  GeV), the correct DM density today, measured by Planck and WMAP arises naturally:

$$\Omega_\chi = \frac{m s_{today} Y_{today}}{\rho_{cr}} \rightarrow \Omega_\chi h^2 \sim \frac{10^{-26} \text{cm}^3/\text{s}}{\langle \sigma v \rangle} \simeq 0.1 \left( \frac{0.01}{\alpha} \right)^2 \left( \frac{m}{100 \text{GeV}} \right) \quad (1.16)$$

This is called the "WIMP miracle" for the theoretical Weak Interacting Massive Particles (WIMPs) which have some candidates within the Super Symmetry (SUSY) theory. While the annihilation of these particles would be strongly suppressed after freeze-out, it can still occur in regions with high DM density. The products of this annihilation are pairs of SM particles that can be detected as an excess signal, giving an indirect evidence of the presence of DM. This is where  $\gamma$ -ray astrophysics takes place: Two DM particles can annihilate directly into a pair of  $\gamma$ -rays with a characteristic line spectrum with  $E_\gamma = m_\chi$  or they can annihilate into pairs of other SM particles which can afterwards decay giving out a continuum spectrum of  $\gamma$ -rays. The differential flux of photons produced by DM annihilation is described as:

$$\frac{d\Phi}{dEd\Omega} = \frac{1}{4\pi} \frac{\langle \sigma v \rangle}{km_{DM}^2} \frac{dN_\gamma}{dE} \int_{l.o.s} dl \rho^2(l, P) \quad (1.17)$$

The first term of the equation comes from the already discussed particle physics, depends on the annihilation channel and the mass of the particle. The integral second term is known as the J-factor and is the integral over the line of sight and solid angle  $\Delta\Omega$  of the squared DM density profile ( $\rho$ ) and it is source dependent. The most simple density profile for a dark matter halo that we can think of is a self-gravitating isothermal gas sphere, where:

$$\rho(r) \propto 1/r^2 \quad (1.18)$$

However, to address the actual physics of galaxy evolution, we need to rely on structure formation simulations which follow the initial DM density perturbations until the formation of current halos. From this simulations and actual observations we know that the DM density profile can be well reproduced as a six-parameters function of distance  $r$  from the center of the profile [48][88][54]:

$$\rho(r) = \frac{\rho_0}{\left(\frac{r}{r_s}\right)^\gamma \left[1 + \left(\frac{r}{r_s}\right)^\alpha\right]^{\frac{\beta-\gamma}{\alpha}}} \Theta(r_{max} - r) \quad (1.19)$$

Where  $\Theta$  is the Heaviside step function,  $r_s$  is the scale radius and  $\rho_0$  is the characteristic density. These two last parameters depend on the specific DM halo. Setting  $(\alpha, \beta, \gamma) = (1, 3, 1)$  we retrieve the Navarro-Frenk-White profile [60]. Combinations of these parameters can be used to fit a possible DM signal to a specific profile.

From 1.17, we state that the best objects to search for a  $\gamma$ -ray signal will be those that are nearby and DM dense, so the J-factor would be sufficiently large relative to the background of  $\gamma$ -rays produced by ordinary matter interactions.

## 1.6 $\gamma$ -ray sources

In the previous section, the processes that produce  $\gamma$ -ray emission were introduced. In this section, the astrophysical objects where they take place are described. Two major classes of  $\gamma$ -ray emitters can be distinguished: galactic sources and extragalactic sources. At the end of the section, potential sources for DM annihilation signals will be also treated. Figure 1.7 show the current known population of VHE  $\gamma$ -ray sources based on the observations of the current generation of  $\gamma$ -ray detectors, either in space (*Fermi*-LAT) or ground based (Major Atmospheric Gamma Imaging Cherenkov Telescopes (MAGIC), High Energy Stereoscopic System (H.E.S.S.), Very Energetic Radiation Imaging Telescope Array System (VERITAS)).

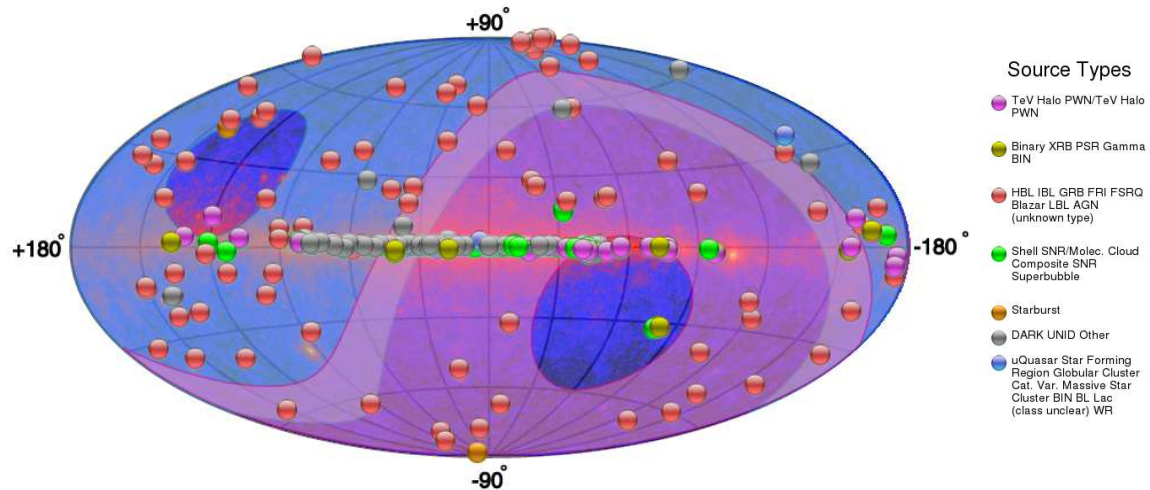


Figure 1.7: Full skymap from TeVCat[84] catalog as of July 2019, with all the detected TeV sources. In the background, the *Fermi*-LAT skymap is shown and the shadowed regions correspond to the MAGIC field of view (blue) and H.E.S.S. (pink).

### 1.6.1 Galactic sources

As shown in figure 1.7, the richest region in  $\gamma$ -ray sources is the galactic plane, meaning that the majority of detected emitters belong to our galaxy. In this section, the different characteristics of these sources will be described.

#### Pulsars

Pulsars are the most common type of  $\gamma$ -ray emitters known. When a massive star ( $< 8M_{\odot}$ ) suffers gravitational core collapse at the end of its life, the resulting object is a compact neutron star sustained by degeneracy pressure, where neutronization (the combination of protons and electrons) has taken place due to the extremely high densities ( $> 10^9 g/cm^3$ ). The neutron star comprises  $1 - 2 M_{\odot}$  in a radius of 10 - 14 km and as the momentum of the parent rotating star is conserved, the much more compact neutron star will spin at extremely high velocities with periods that can go from milliseconds to a few seconds. This fast spin produces strong magnetic fields in their surroundings. When the magnetic fields are aligned with the line of sight from the Earth, we can detect a pulsed emission with a period as of the rotation of the neutron star, and this is called pulsar. The pulsed emission has been detected

in many wavelengths, either radio, optical, X-ray and also in  $\gamma$ -rays.

It is generally accepted that the origin of the  $\gamma$ -ray emission from pulsars is due to curvature radiation, produced when relativistic electrons accelerated in gaps of the electromagnetic fields powered by the pulsar rotation, get trapped along the lines of the magnetic field [22]. However, the location of the gaps and the acceleration mechanism which dominates is not well known and there are different models proposed (see figure 1.8).

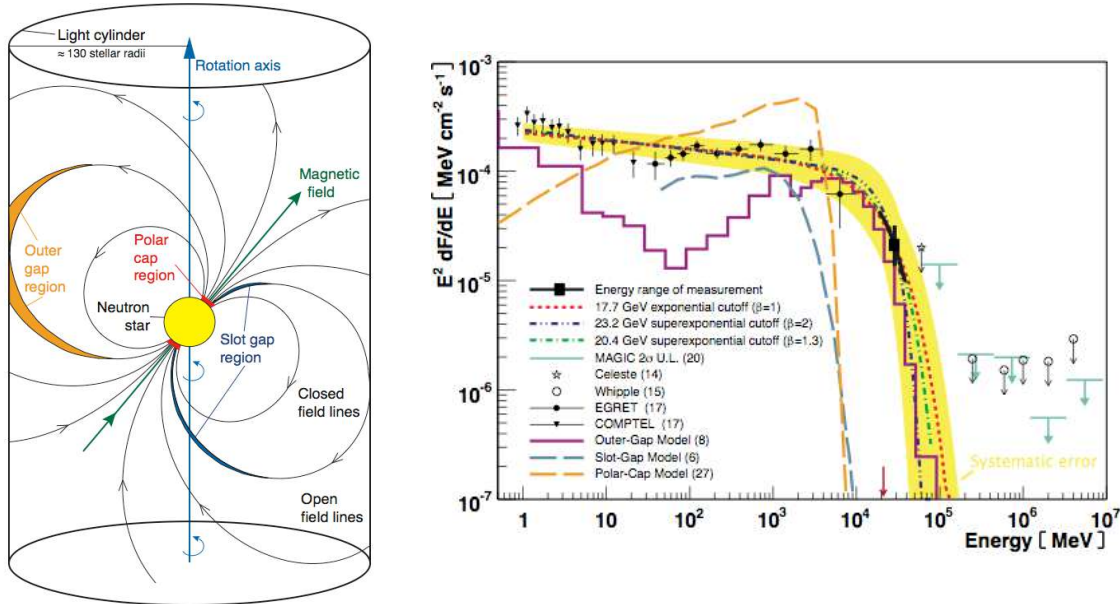


Figure 1.8: *Left:* Crab pulsar's magnetosphere where the location of the three models (Polar-Cap in red, Slot-Gap in blue and Outer-Gap in yellow) is shown. *Right:* Crab pulsar spectral cutoff. Figures from [22]

Combined observations of the Crab pulsar from the Imaging Compton Telescope (COMPTEL), the Energetic Gamma Ray Experiment Telescope (EGRET) [56] and the MAGIC [22] has shown that their power law spectrum presents a cutoff at energies over a few GeV (see figure 1.8). The detection of the pulsar emission at energies over 25 GeV by MAGIC ruled out the possibility of acceleration happening too close to the pulsar (as the Polar-Cap model assets) because the magnetic pair-production attenuation would provide a super-exponential cutoff at much lower energies to those observed. Current predictions of the Outer-Gap model best explains the observed Crab pulsar spectrum up to date [50].

While pulsars are the most common  $\gamma$ -ray emitters, only two have been detected in the VHE range, up to TeV energies: the Crab and Vela pulsars [41].

### Supernova Remnants

Supernovae are the result of the evolution of a star, which suddenly becomes much brighter while shells of gas are expelled off back to the interstellar medium in an explosive event. They can be classified in different types by features in their spectrum which also implies a different origin of the explosion. Type II supernovae show hydrogen emission lines, meaning they come from very massive stars ( $M > 8M_\odot$ ) with hydrogen in their outer layers. After

burning lighter elements (H, He, etc.) into heavy nuclei, fusion reactions become inefficient and the imbalance between gravitational forces and pressure radiation lead to the collapse of the central core into a neutron star or a black hole in a violent reaction, expelling shells of material at high velocities. Type I supernovae do not present hydrogen lines, meaning they come from an hydrogen-poor star. They usually are produced by white dwarfs in binary systems which accrete material until reaching the Chandrasekhar limit [28] and suffer a thermonuclear explosion. Type Ia have Si lines in their spectra. Those type I without Si lines are classified as Ib if they have He lines and Ic if they do not [64].

The structure of ejected material which is left in the surroundings of the parent star is the SNR. They can be classified in different types depending on their spectrum, but the most important feature to differentiate them is the presence (or not) of a shell. There are shell-type SNR, in which the material in the surroundings is heated by the power of the shockwave during the SN explosion. The named "plerion" SNR or PWN do not present a shell. Their emission is produced by the interaction between electrons ejected to the medium by a central pulsar and its huge magnetic field. There is also a composite type of SNR where a plerion is surrounded by a shell and depending on the wavelength observed, they emit more like one type or the other [85].

Depending on the SNR type, the particle acceleration and  $\gamma$ -ray emission would have a different origin and features.

- **Shell-type remnants:** Shell-type remnants, commonly referred simply as SNR, are the most clear candidates for CR acceleration. Finding evidence for this hypothesis is difficult due to the deflection of CRs by magnetic fields in the ISM which makes it impossible to trace back the emission direction. Neutral particles, like neutrinos and  $\gamma$ -rays can be used as tracers of CR acceleration. We know CRs can produce  $\gamma$ -rays via hadronic interactions with the gas and dust in the medium. For example, the production of pions and posterior pion decay would give a spectrum with a characteristic peak at 67.5 MeV.

As a rough estimation, if we assume that the typical total kinetic energy produced by a SN explosion is around  $E_{SN} \sim 10^{51}$  erg, with a SN rate in the galaxy of about one in 50-100 years, and a constant fraction  $\eta$  of the kinetic energy is transferred to hadrons, it can be shown that this fraction has to be of the order of the 10% to retrieve the approximated CR luminosity in the galaxy  $L_{CR} \sim 2 \times 10^{41}$  erg/s.

$$L_{CR} = \eta \cdot E_{SN} \cdot SN_{rate} = 0.1 \cdot 10^{51} \text{ erg} \cdot 50 \text{ yr}^{-1} \propto 10^{41} \text{ erg/s} \quad (1.20)$$

A more detailed analysis using real data of galactic SNR was done by [25] arriving at the conclusion that future  $\gamma$ -ray data can be used to constrain the amount of CR energy coming from SNR. However, there are still problems on proving this hypothesis because many of the  $\gamma$ -ray signatures coming from SNR have a leptonic origin rather than hadronic. Also a cut-off is observed before the knee region so only small diffusion coefficients could describe the observed CR spectrum.

- **Plerions or Pulsar Wind Nebulae.** Pulsar Wind Nebulae (PWNe) are a type of SNR where instead of having a shell-like emission, a cloud of highly magnetized material is powered by a central pulsar. The rotating pulsar dissipates kinetic energy over time in the form of "spin down luminosity", and injects it steadily into the surrounding

nebula of ejected material during stellar evolution. To understand the features of the emission of PWNe, it is important to follow their evolution with time and how the period, spin down luminosity and magnetic field changes [40]. A pulsar is formed in a SN explosion and the final state of the pulsar and its PWN will depend on how it interacts with the SNR. If the SNR expands outward freely, the pulsar will remain in the center, but if a reverse shock happens, reverberations between the PWN and the shock can produce instabilities which in the end will displace the pulsar from its original position, even being able to cross away the SNR shell.

Strong magnetic fields in pulsars create currents of particles of the surrounding nebula, producing pulsar winds. Electrons accelerated this way produce synchrotron radiation from radio to X-ray wavelengths. The wind starts decelerating when reaching the nebula radius, due to the more slowly expanding material and thus a wind termination shock is formed. The TeV  $\gamma$ -ray emission from PWNe is explained as IC emission produced by the relativistic particles in the shocked wind interacting with the synchrotron photons. The Crab PWNe was the first source detected of this type, associated with a SN explosion observed in 1054CE, and has become a sort of standard candle for  $\gamma$ -ray astrophysics.

- **Composite remnants.** The third type of SNR is a combination of the previous two, where a PWN is surrounded by a shell-type SNR. Examples of this kind would be SNRs W28 or W44.

### **$\gamma$ -ray binaries**

$\gamma$ -ray binaries are systems composed by two objects orbiting each other: One is a compact object, such as a pulsar and the other can be an ordinary massive star big enough to reach the Roche lobe of the pulsar and so stellar winds connect the two objects. Just a few objects ( $\sim 10$ ) of this kind have been detected in VHE  $\gamma$ -rays very recently, and yet the exact mechanisms of the origin of their emission are unknown. There are two main explanations to the HE and VHE emission in  $\gamma$ -ray binaries. It can be produced by accretion energy released in the form of relativistic jets, or on the other hand, by the energy emitted by the pulsar in the form of pulsar winds in a similar way as in PWNe. The first case is denominated the *microquasar* scenario due to its similarities with AGNs (also known as quasars) but emitting jets in a smaller scale. However, a variety of indirect evidences seem to favour the pulsar wind interpretation mainly based in the spectral similarities of the known binaries with the power of a pulsar spindown. Also the presence of strong magnetic fields and morphological characteristics of radio emission are similar features to those found in PWNe [36].

### **Novae**

Binary star systems are rather common objects in the universe. One of the stars can be more massive than the other, evolving faster and becoming a white dwarf while the second star can still be in its main sequence phase. If this happens, the white dwarf can start to attract material from the companion, building an accretion disk. The hydrogen rich gas in the surface of the white dwarf starts heating in the bottom layers and become electron-degenerate, leading to a chain of thermonuclear explosions [31]. This event is known as "classical nova". When the companion star is a red giant, which has highly increased its volume, the system

is called a *symbiotic binary system*. In this case, the interaction between the stellar wind of the red giant and the white dwarf surface expansion give place to a favorable scenario for particle acceleration. Both classical novae and symbiotic systems have been detected in HE  $\gamma$ -rays by *Fermi*-LAT [4], [14] although their results where not able to differentiate which emission scenario is taking place. In the hadronic scenario, the  $\gamma$ -ray emission would be produced by high energy protons interacting with nuclei to produce neutral pions in the stellar winds of the binary system. In the leptonic scenario, accelerated electrons would produce  $\gamma$ -rays through a combination of ic scattering and bremsstrahlung in the proximity of the nova [76].

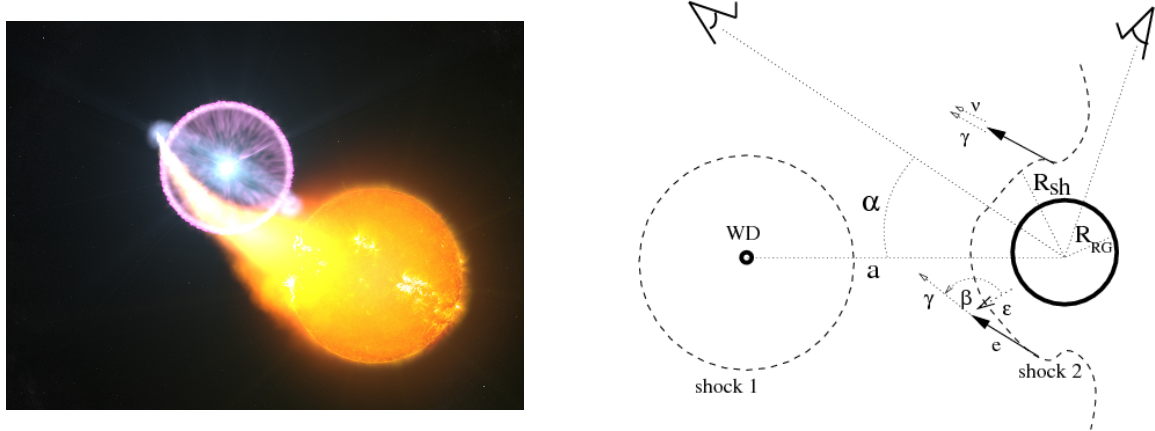


Figure 1.9: *Left:* Artist concept of a classical nova. Credits: NASA’s Goddard Space Flight Center/S. Wiessinger. *Right:* Diagram of the geometry of the symbiotic binary system V407 Cyg from [76]. The expanding shock (1) from the white dwarf partially overtakes the Red Giant (shock 2), producing particle acceleration through ic (leptonic scenario, with angle of interaction  $\beta$ ) and proton collisions with the red giant wind (hadronic scenario).

### The Galactic Center and the *Fermi* Bubbles

The center of the Milky Way, known as the Galactic Center (GC) is a region of the sky situated at  $4^\circ$  longitude,  $2^\circ$  latitude, with a size of  $600 \times 300$  pc and at a distance of about 8 kpc. It has been observed in all wavelengths, and while it is obscured by dust in the optical and ultraviolet range, emission in infrared radio, X-rays and  $\gamma$ -rays reveals a prolific region full of energetic sources. Among many SNRs, PWNe and stellar clusters in HII regions, there is also a Super Massive Black Hole (SMBH), Sagittarius A\*, whose detection has been one of the major motivations for GC surveys. Possibly closely related to Sgr A\* (but still not confirmed) are the *Fermi bubbles*, two large  $\gamma$ -ray lobes that appear to be ejected from the center of the galaxy.

The GC has been surveyed by many  $\gamma$ -ray experiments (*Fermi*-LAT, MAGIC, H.E.S.S.) and emission from HE to VHE bands has been detected. The main problem with this highly populated region is the difficulty of tell apart individual sources, making it a big challenge to identify the actual emission from Sgr A\* [43]. The high energy emission from Sgr A\* has its origin in the strong winds produced by the presence of an accretion disk surrounding the

black hole, where material is accelerated at very high energies [44].

The Fermi bubbles were discovered while searching for a  $\gamma$ -ray counterpart to the WMAP haze [79], which is a residual microwave emission that arises after subtracting all the other known emission components. They extend to  $55^\circ$  up and above the GC and are not symmetric, with an enhanced emission towards the south-east side of the bubbles. With well defined edges, an uniform power-law spectrum of index  $\sim 2$  and a cocoon-like shape, they resemble jet-like structure [18]. Their origin is still under debate: They could be jets, outflows or the result of accretion events from the black hole, winds from SN explosions or the remnant of AGN activity in the Milky Way in the past.

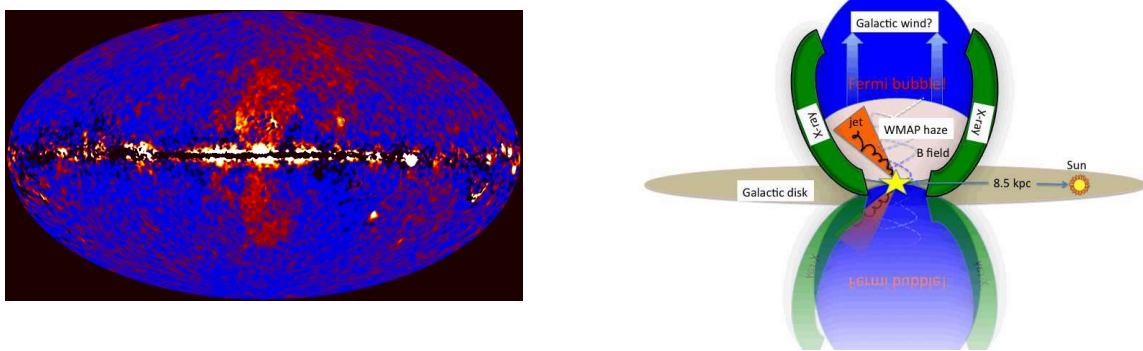


Figure 1.10: *Left:* Fermi Bubbles as seen by *Fermi*-LAT after subtracting all the other known  $\gamma$ -ray components. Credits: NASA/DOE/*Fermi* LAR/D. Finkbeiner et al. *Right:* Schematic picture of Fermi Bubbles structure from [79].

### Globular Clusters

Globular clusters are compact gravitationally bounded stellar associations with spherical geometry which are distributed outside the galactic plane, conforming a spherical halo around the galaxy. They are old highly evolved systems with many compact objects like neutron stars, white dwarfs and pulsars even forming binary systems. Furthermore, the majority ( $\sim 80\%$ ) of Millisecond Pulsars (MSPs) (pulsars with a period of the order of milliseconds) detected up to date have been found in globular clusters.

Since all the mentioned objects are well known  $\gamma$ -ray emitters, globular clusters have been observed and detected in *gamma*-rays by *Fermi*-LAT [1] and H.E.S.S. [45]. Even pulsed  $\gamma$ -ray emission have been observed from individual MSPs [39], [86]. Two types of models of  $\gamma$ -ray emission have been discussed to happen in globular clusters, both related to MSPs. One takes place in MSPs magnetospheres, where  $\gamma$ -ray emission would be produced by curvature radiation. The second type of models involve scattering of electrons accelerated close to the MSP with optical, infrared or CMB photons [80].

## 1.6.2 Extragalactic sources

While most of the  $\gamma$ -ray emission detected on Earth comes from the galactic plane, there is a big amount of individual sources outside our galaxy which produce HE radiation and allow the study of a new range of extragalactic phenomena. A big caveat for extragalactic sources

is that the VHE range is suppressed by the EBL absorption, as described in section 1.4.

### Active Galactic Nuclei

AGN are the brightest steady sources of  $\gamma$ -ray in the universe. They are galaxies with luminosities much stronger than those which will be produced by nuclear reactions in stars. Their strong emission, concentrated in a very small volume is powered by a SMBH located in the center of the galaxy [81]. The Black Hole (BH) attracts gas and material from the galaxy forming an accretion disk, where matter loses angular momentum through viscous and turbulent processes, and emits a huge amount of energy from ultraviolet to soft X-ray bands. AGN can be classified in two broad types, according to their radio emission: *Radio-quiet* and *radio-loud*. Radio-loud AGN (also known as Blazars) have the greatest  $\gamma$ -ray emission, because they form jets ejected from the BH perpendicular to the accretion disk, where particles are accelerated to ultrarelativistic energies in the presence of strong magnetic fields. They are hosted by giant spiral galaxies which are believed to be the result of recent galaxy merging. When the jets are pointing towards the Earth, these AGN are observed as a variable source with a certain period. Blazars are the most common type of AGN detected in  $\gamma$ -rays, with more than 1500 sources detected at GeV energies, and more than 60 at TeV energies. They have cosmological importance because VHE observations of high redshift blazars can test the transparency of the universe, setting limits to the EBL density and thus giving information on the star formation rates along the evolution of the universe.

Actually, the classification of different types of AGN further than their radio emission, depend strongly on their orientation. Different orientation angles can make AGN appear as spectroscopically completely different sources, depending on the region of the object that is showing. All AGN have a dusty tori, broad-line regions, narrow-line regions and strong blue/UV bump emissions from the accretion disk [34]. Depending on the angle, one or several of these regions will be observable and will show their particular features in the spectrum. Figure 1.11 show a scheme of AGNs taxonomy.

### Gamma Ray Bursts

GRBs are short and intense flashes of  $\gamma$ -ray emission coming isotropically from random directions in the sky. With a range of luminosities from  $10^{51} \text{ ergs/cm}^2$  to  $10^{52} \text{ ergs/cm}^2$  they are the brightest transient objects in the sky [68], emitting in just seconds the same amount of energy radiated in years by a galaxy like the Milky Way. They can last from just a few seconds (short GRBs) to several hours (ultra-long GRBs), being the most common the ones that last for few minutes (long GRBs). Long bursts are usually followed by afterglows in X-rays, optical and radio which can last for several years after the event.

The so called *fireball* model is the generally accepted mechanism which drives GRB. Since the observed emission of the bursts is not thermal, its origin must be the result of the conversion of an ultra-relativistic energy flow into radiation in an optically thin region. The energy flow could come from the kinetic energy of accelerated particles or electromagnetic Poynting flux [67]. In this model, the process is ignited by an "inner engine" which is not possible to observe directly, but which activity can be characterized by the observed temporal structure of the bursts. The engine produces an explosive fireball of the size of the engine itself. There is an alternative model based in internal shocks, where the engine would produce a wind

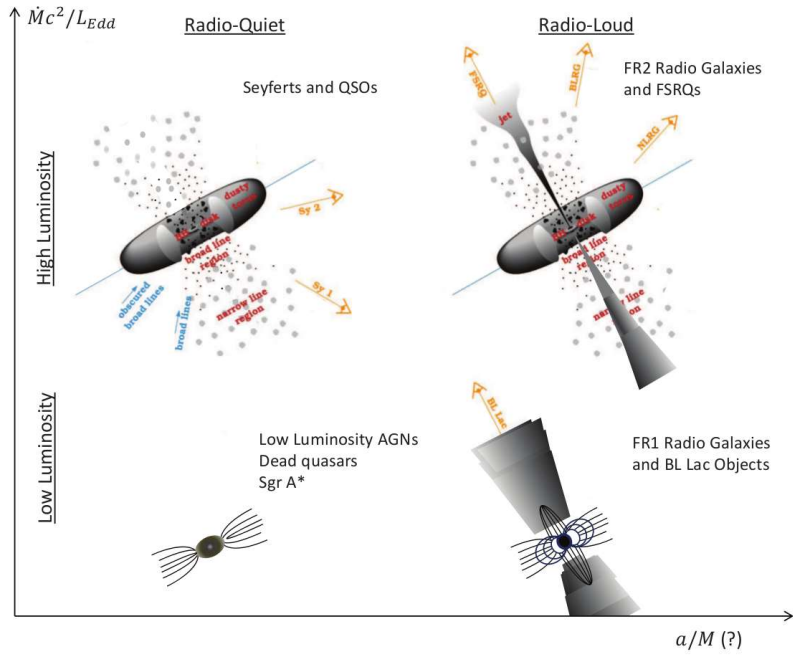


Figure 1.11: AGN taxonomy as from [34]. In this scheme, the vertical axis represents the luminosity power in terms of the mass-accretion rate and horizontal axis represents the BH rotation.

and a long energy flow. About the nature of the phenomena producing GRBs, there exist an apparent difference between the origin of short GRB and long GRB according on their hardness ratio (defined as the ratio of the flux in two separated bands) versus duration plot (see figure 1.12) [53].

These two populations in the hardness ratio vs. duration plot, together with rather significant spectral differences [42] and afterglow observations, suggest that long GRBs are closely related to star forming regions, compatible with SN explosions of massive stars. Short GRBs on the other hand, could be related to more evolved regions and be the result of neutron star mergers.

Many GRBs have been detected in HE and recently MAGIC, which were specifically designed to observe such objects, detected the first event in the VHE range [59].

### Starburst galaxies

Starburst galaxies are those with a greatly enhanced star formation, whose Star Formation Rate (SFR) is considered to be out of equilibrium, consuming gas for star formation at very short timescales ( $< 1$  Gyr). Since the SFR is highly correlated with the SN explosion rate, it is expected that  $\gamma$ -ray emission detected from starburst galaxies has its origin in SNRs. The production and transport of CRs in the ISM significantly affects the star formation, because CRs penetrate deep into molecular cloud cores (molecular clouds are dense gas regions where star formation takes place) catalyzing complex chemical reactions which can affect the initial conditions of star formation and evolution [62]. The conditions of the ISM

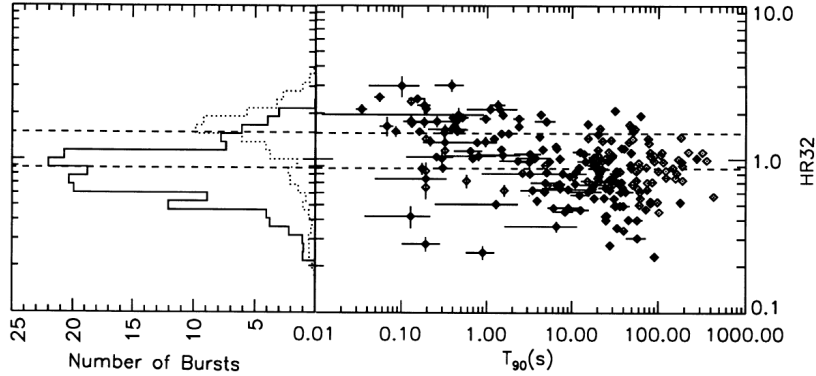


Figure 1.12: *Left:* Hardness ratios for the two duration classes of GRB. Solid lines corresponds to short GRBs, dashed line to long GRBs. *Right:* Hardness vs. duration plot, where duration  $T_{90}$  is defined as the time during which the cumulative counts  $> 25$  keV increase from 5% to 95% above background. Dashed lines correspond to the mean hardness ratio of the two classes. Figure from [53].

in starburst galaxies are very different from Milky Way. The gas density is much higher and the high population of massive stars produce a huge amount of radiation, which is absorbed by dust and re-emitted in infrared. Magnetic fields are also affected by the presence of such population. Thereby particles accelerated in the region will suffer strong losses of energy and faster cooling. Detection of  $\gamma$ -rays from starburst galaxies is a key probe to understand the efficiency of CR acceleration in SNRs and CR transport in different ISMs.

The current generation of  $\gamma$ -ray telescopes have detected NGC253 and M82 starburst galaxies ([11], [83], [2]), which has been long predicted to emit  $\gamma$ -rays up to VHE range.

### Galaxy clusters

Galaxy clusters are the largest gravitationally bounded structures in the universe. They are mainly composed of DM (70-80% of the total mass) and their ordinary matter is composed by the galaxies and the filaments connecting them, plus a big amount of hot gas in the surroundings called the Intracluster Medium (ICM). In the standard paradigm of structure formation, clusters are formed by hierarchical mergers and accretion of smaller structures. Mergers are the most energetic phenomena to occur in the universe (they release  $10^{63}$ - $10^{64}$  ergs/Gyr) and they dissipate energy in the form of shocks which heat the gas, or through large-scale ICM motions [26]. Part of the energy dissipated during this process is fused into particle acceleration to ultra-relativistic energies, thus they are a source of CR production. Radio observations of galaxy clusters proves the existence of non thermal emission from synchrotron radiation processes in the ICM. Galaxy clusters can therefore be a source of HE photons which can be produced via leptonic scenario through ic scattering of CMB photons with ultra-relativistic electrons, or hadronic scenario by neutral pion decay.

Until recently,  $\gamma$ -ray experiments that tried to detect  $\gamma$ -ray signal from the closest galaxy clusters were only able to set upper limits [15], [21]. *Fermi*-LAT was able to report a detection of an extended  $\gamma$ -ray signal from the Coma cluster roughly correlated with the radio halo [87].

### Neighbour galaxies

The Local Group is the cluster of galaxies gravitationally bounded to the Milky Way. They are the closest galaxies to be observed and their characteristics are expected to be similar to those of our own galaxy. The second and third closest and spatially resolved galaxies (the first being the Canis Major dwarf galaxy) are the Large Magellanic Cloud (LMC) and the Small Magellanic Cloud (SMC). They are two irregular dwarf galaxies seen in the southern hemisphere, at a distance of 50 kpc [33]. They present a remarkable high star formation rate ( $\sim 0.2\text{yr}^{-1}$  for the LMC,  $0.3\text{yr}^{-1}$  for the SMC [70], compared to the  $0.68\text{yr}^{-1}$  to  $1.45\text{yr}^{-1}$  of the Milky Way [71] in a much smaller volume.) so it is expected that  $\gamma$ -rays produced by interaction of CR with ISM can be detected from the Magellanic Clouds.

The first detection of a  $\gamma$ -ray diffuse signal from the LMC was made by EGRET [78], being the first normal galaxy outside the Milky Way detected in  $\gamma$ -rays. The SMC was first detected in  $\gamma$ -rays by *Fermi*-LAT [3]. Further observations of the LMC from *Fermi*-LAT at HE [6], [13], [32] and H.E.S.S. [46], [52] at VHE revealed a complex structure of the diffuse emission and a population of very interesting individual sources comprising pulsars, SNRs,  $\gamma$ -ray binaries... Since the LMC emission in  $\gamma$ -rays is one of the main topics of this thesis, it will be extensively treated in chapter ??.

Apart from the before mentioned starburst galaxies M82 and NGC253, other close galaxies such as M31 and M33 have also been observed and detected in HE  $\gamma$ -rays by *Fermi*-LAT [16].

### 1.6.3 Potential Dark Matter annihilation emission sources

In section 1.5 the production of  $\gamma$ -rays through WIMP annihilation or decay was described. In the search for this kind of signal, one can analyze which would be the best sources in the universe for an indirect search of DM. First of all, they must have a high amount of DM, given by the astrophysical parameter J-factor (integral term in eq. 1.17). Also, a low background of other  $\gamma$ -ray sources would allow to unequivocally identify the DM signal. Following these premises, indirect DM searches have been performed by  $\gamma$ -ray experiments in the most promising sources:

### Milky Way Galactic Center

In the present evolutionary stage of the universe, galaxies are believed to be embedded in DM halos which extend much more than the visible matter, the center of the galaxies being the location of higher DM density [61]. The center of the Milky Way is therefore a promising target for DM searches. However, as explained in section 1.6.1, it is also a very populated region with a lot of  $\gamma$ -ray sources which are even not fully resolved. This fact makes the GC a true challenge for disentangle a possible DM emission, needing a very good background modelling and control of the instrumental systematics [29]. Usually, DM searches in the GC tend to avoid the galactic plane region, observing a region with lower background at expenses of having a weaker DM signal due to the lower density.

The most constraining upper limits in the VHE energy range for the velocity averaged cross section  $<\sigma v>$  in the GC have been established by H.E.S.S. [7]. Both *Fermi*-LAT and H.E.S.S. have accounted for a  $\gamma$ -ray excess coming from the GC of unknown origin which

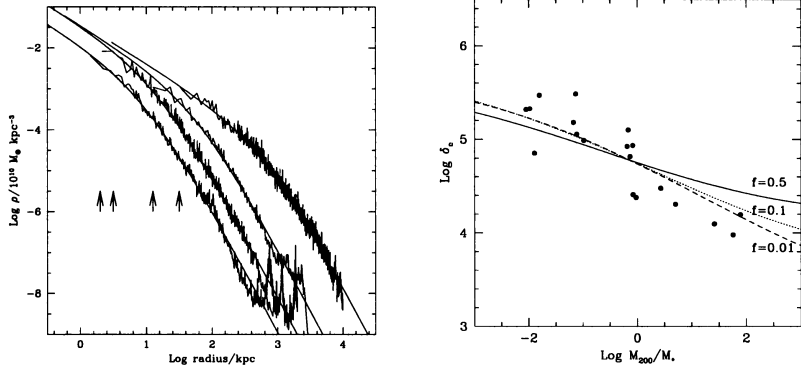


Figure 1.13: *Left:* Typical density profiles from CDM halos obtained from N-body simulations. *Right:* Characteristic overdensity of halos as a function of mass. Masses are expressed in units of the current non linear mass corresponding to the standard biased CDM spectrum  $M_* = 3.3 M_\odot$ . Figures from [61].

has been tried to be fitted with the most conventional DM models, but the results were not sufficiently compatible [19], [17].

### Dwarf Spheroidal Galaxies and Dark Clumps

Following the standard model of cosmology, N-body simulations of the evolution of CDM since the Big Bang predicts a hierarchical structure formation where DM clusters into subhalos which merge into higher structures. The final picture at galactic scales, are galaxies embedded in a big DM halo, surrounded by a population of subhalos which mass is inversely proportional to their number [55]. Simulations like Via Lactea II predict that the Milky Way is surrounded by a large number of DM subhalos ( $\sim 50,000$ ). The heavier of these substructures are the so called Dwarf Spheroidal Galaxies (DSphe). They are very faint galaxies (in optical) orbiting the Milky Way. Many of the observed DSphes are strongly DM dominated, but have absent or very little star formation and no signal of ionized or neutral gas [75]. Smaller structures with no emission at all are known as Dark Clumps.

These kind of objects are a perfect target for DM searches because no  $\gamma$ -ray signal is expected from them due to ordinary astrophysical processes. Any  $\gamma$ -ray detection would be an unequivocal signal of DM annihilation.

The "missing satellites problem" accounts for the discrepancy between the large number of predicted subhalos by simulations and the actual number of detected DSphes ( $\sim 50$ ) hence the study and understanding of these objects could set strong boundaries to the CDM model or even drive to other DM models like *warm* dark matter.

The present generation of  $\gamma$ -ray experiments have widely studied this objects in the search for DM, not yet being succesful at detection but setting upper limits for many known DSphes [5], [9],[20], [24] .

### Galaxy Clusters

As has been mentioned before in section 1.6.2, galaxy clusters are mostly dominated by DM with a very high mass-to-light ratio. For this reason, they are good targets for indirect DM

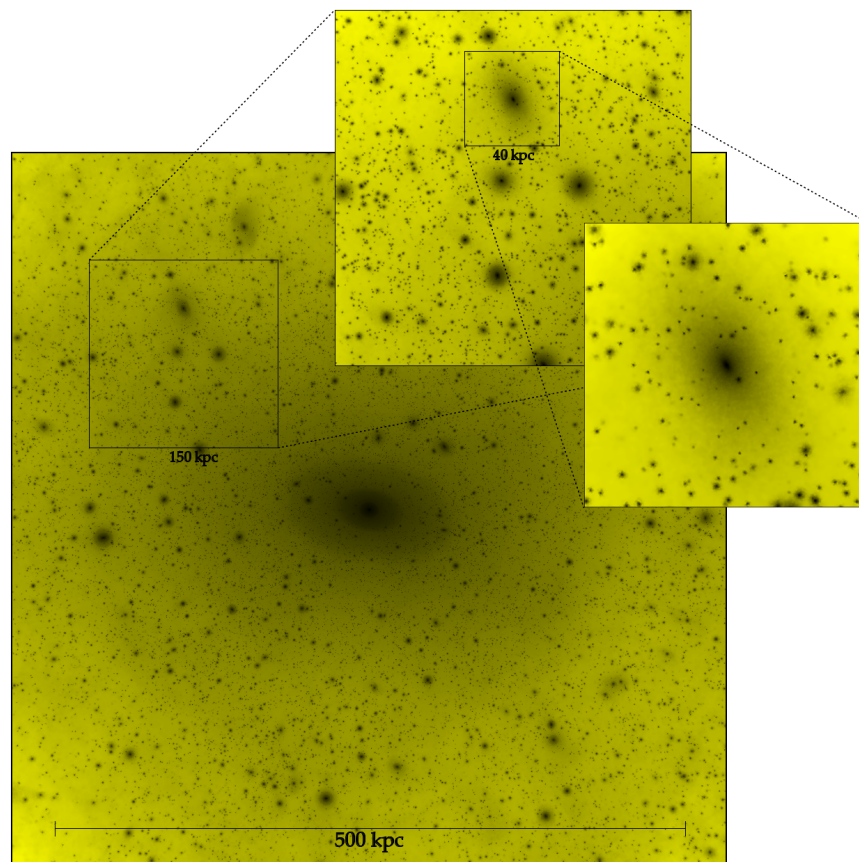


Figure 1.14: Results from *Via Lactea* N-body simulations of DM substructures. The picture show a projection of density squared in a  $566 \text{ kpc} \times 566 \text{ kpc} \times 566 \text{ kpc}$  region centered on the host halo at  $z = 0$ , from [55].

searches both for annihilation and decay. They are specially suitable for decaying DM, since at large volumes the signal of decaying DM which is proportional to the first power of the density overshines the signal of annihilation [30].

Strong constraints for a wide number of models for DM annihilation and decay have been set by *Fermi*-LAT [51], [12] and H.E.S.S. [8], and also constraints on the decaying lifetime of DM were set by MAGIC [10].

### The Large Magellanic Cloud

The LMC has been considered a well promising target for DM searches due to its proximity and rather high J-factor ( $10^{20} J/GeV^2 cm^{-5}$ ). Kinematic studies of the LMC show that more than half of the LMC mass is forming a dark halo with a compact central bulge [82], [77].

*Fermi*-LAT has used five years of data to set constraints on the DM annihilation signal from the LMC in the HE regime [27]. No limits has yet been set in the VHE range though. As one of the main topics of this thesis, more on this subject will be extensively discussed in chapter ??.





## Bibliography

- [1] A. A. Abdo et al. “A population of gamma-ray emitting globular clusters seen with the Fermi Large Area Telescope”. In: *Astronomy and Astrophysics* 524, A75 (Dec. 2010), A75. DOI: [10.1051/0004-6361/201014458](https://doi.org/10.1051/0004-6361/201014458). arXiv: [1003.3588 \[astro-ph.GA\]](https://arxiv.org/abs/1003.3588).
- [2] A. A. Abdo et al. “Detection of Gamma-Ray Emission from the Starburst Galaxies M82 and NGC 253 with the Large Area Telescope on Fermi”. In: *Astrophysical Journal* 709.2 (Feb. 2010), pp. L152–L157. DOI: [10.1088/2041-8205/709/2/L152](https://doi.org/10.1088/2041-8205/709/2/L152). arXiv: [0911.5327 \[astro-ph.HE\]](https://arxiv.org/abs/0911.5327).
- [3] A. A. Abdo et al. “Detection of the Small Magellanic Cloud in gamma-rays with Fermi/LAT”. In: *Astronomy and Astrophysics* 523, A46 (Nov. 2010), A46. DOI: [10.1051/0004-6361/201014855](https://doi.org/10.1051/0004-6361/201014855). arXiv: [1008.2127 \[astro-ph.HE\]](https://arxiv.org/abs/1008.2127).
- [4] A. A. Abdo et al. “Gamma-Ray Emission Concurrent with the Nova in the Symbiotic Binary V407 Cygni”. In: *Science* 329.5993 (Aug. 2010), pp. 817–821. DOI: [10.1126/science.1192537](https://doi.org/10.1126/science.1192537). arXiv: [1008.3912 \[astro-ph.HE\]](https://arxiv.org/abs/1008.3912).
- [5] A. A. Abdo et al. “Observations of Milky Way Dwarf Spheroidal Galaxies with the Fermi-Large Area Telescope Detector and Constraints on Dark Matter Models”. In: *Astrophysical Journal* 712.1 (Mar. 2010), pp. 147–158. DOI: [10.1088/0004-637X/712/1/147](https://doi.org/10.1088/0004-637X/712/1/147). arXiv: [1001.4531 \[astro-ph.CO\]](https://arxiv.org/abs/1001.4531).
- [6] A. A. Abdo et al. “Observations of the Large Magellanic Cloud with Fermi”. In: *Astronomy and Astrophysics* 512, A7 (Mar. 2010), A7. DOI: [10.1051/0004-6361/200913474](https://doi.org/10.1051/0004-6361/200913474). arXiv: [1001.3298 \[astro-ph.HE\]](https://arxiv.org/abs/1001.3298).
- [7] A. Abramowski et al. “Search for a Dark Matter Annihilation Signal from the Galactic Center Halo with H.E.S.S.” In: *Physical Review Letters* 106.16, 161301 (Apr. 2011), p. 161301. DOI: [10.1103/PhysRevLett.106.161301](https://doi.org/10.1103/PhysRevLett.106.161301). arXiv: [1103.3266 \[astro-ph.HE\]](https://arxiv.org/abs/1103.3266).

- [8] A. Abramowski et al. “Search for Dark Matter Annihilation Signals from the Fornax Galaxy Cluster with H.E.S.S.” In: *Astrophysical Journal* 750.2, 123 (May 2012), p. 123. DOI: [10.1088/0004-637X/750/2/123](https://doi.org/10.1088/0004-637X/750/2/123). arXiv: [1202.5494 \[astro-ph.HE\]](https://arxiv.org/abs/1202.5494).
- [9] A. Abramowski et al. “Search for dark matter annihilation signatures in H.E.S.S. observations of dwarf spheroidal galaxies”. In: *Physical Review D* 90.11, 112012 (Dec. 2014), p. 112012. DOI: [10.1103/PhysRevD.90.112012](https://doi.org/10.1103/PhysRevD.90.112012). arXiv: [1410.2589 \[astro-ph.HE\]](https://arxiv.org/abs/1410.2589).
- [10] V. A. Acciari et al. “Constraining dark matter lifetime with a deep gamma-ray survey of the Perseus galaxy cluster with MAGIC”. In: *Physics of the Dark Universe* 22 (Dec. 2018), pp. 38–47. DOI: [10.1016/j.dark.2018.08.002](https://doi.org/10.1016/j.dark.2018.08.002). arXiv: [1806.11063 \[astro-ph.HE\]](https://arxiv.org/abs/1806.11063).
- [11] F. Acero et al. “Detection of Gamma Rays from a Starburst Galaxy”. In: *Science* 326.5956 (Nov. 2009), p. 1080. DOI: [10.1126/science.1178826](https://doi.org/10.1126/science.1178826). arXiv: [0909.4651 \[astro-ph.HE\]](https://arxiv.org/abs/0909.4651).
- [12] M. Ackermann et al. “Constraints on dark matter annihilation in clusters of galaxies with the Fermi large area telescope”. In: *Journal of Cosmology and Astroparticle Physics* 2010.5, 025 (May 2010), p. 025. DOI: [10.1088/1475-7516/2010/05/025](https://doi.org/10.1088/1475-7516/2010/05/025). arXiv: [1002.2239 \[astro-ph.CO\]](https://arxiv.org/abs/1002.2239).
- [13] M. Ackermann et al. “Deep view of the Large Magellanic Cloud with six years of Fermi-LAT observations”. In: *Astronomy and Astrophysics* 586, A71 (Feb. 2016), A71. DOI: [10.1051/0004-6361/201526920](https://doi.org/10.1051/0004-6361/201526920). arXiv: [1509.06903 \[astro-ph.HE\]](https://arxiv.org/abs/1509.06903).
- [14] M. Ackermann et al. “Fermi establishes classical novae as a distinct class of gamma-ray sources”. In: *Science* 345.6196 (Aug. 2014), pp. 554–558. DOI: [10.1126/science.1253947](https://doi.org/10.1126/science.1253947). arXiv: [1408.0735 \[astro-ph.HE\]](https://arxiv.org/abs/1408.0735).
- [15] M. Ackermann et al. “GeV Gamma-ray Flux Upper Limits from Clusters of Galaxies”. In: *Astrophysical Journal* 717.1 (July 2010), pp. L71–L78. DOI: [10.1088/2041-8205/717/1/L71](https://doi.org/10.1088/2041-8205/717/1/L71). arXiv: [1006.0748 \[astro-ph.HE\]](https://arxiv.org/abs/1006.0748).
- [16] M. Ackermann et al. “Observations of M31 and M33 with the Fermi Large Area Telescope: A Galactic Center Excess in Andromeda?” In: *Astrophysical Journal* 836.2, 208 (Feb. 2017), p. 208. DOI: [10.3847/1538-4357/aa5c3d](https://doi.org/10.3847/1538-4357/aa5c3d). arXiv: [1702.08602 \[astro-ph.HE\]](https://arxiv.org/abs/1702.08602).
- [17] M. Ackermann et al. “The Fermi Galactic Center GeV Excess and Implications for Dark Matter”. In: *Astrophysical Journal* 840.1, 43 (May 2017), p. 43. DOI: [10.3847/1538-4357/aa6cab](https://doi.org/10.3847/1538-4357/aa6cab). arXiv: [1704.03910 \[astro-ph.HE\]](https://arxiv.org/abs/1704.03910).
- [18] M. Ackermann et al. “The Spectrum and Morphology of the Fermi Bubbles”. In: *Astrophysical Journal* 793.1, 64 (Sept. 2014), p. 64. DOI: [10.1088/0004-637X/793/1/64](https://doi.org/10.1088/0004-637X/793/1/64). arXiv: [1407.7905 \[astro-ph.HE\]](https://arxiv.org/abs/1407.7905).
- [19] F. Aharonian et al. “HESS Observations of the Galactic Center Region and Their Possible Dark Matter Interpretation”. In: *Physical Review Letters* 97.22, 221102 (Dec. 2006), p. 221102. DOI: [10.1103/PhysRevLett.97.221102](https://doi.org/10.1103/PhysRevLett.97.221102). arXiv: [astro-ph/0610509 \[astro-ph\]](https://arxiv.org/abs/astro-ph/0610509).

- [20] M. L. Ahnen et al. “Indirect dark matter searches in the dwarf satellite galaxy Ursa Major II with the MAGIC telescopes”. In: *Journal of Cosmology and Astroparticle Physics* 2018.3, 009 (Mar. 2018), p. 009. DOI: 10.1088/1475-7516/2018/03/009. arXiv: 1712.03095 [astro-ph.HE].
- [21] J. Aleksić et al. “Constraining cosmic rays and magnetic fields in the Perseus galaxy cluster with TeV observations by the MAGIC telescopes”. In: *Astronomy and Astrophysics* 541, A99 (May 2012), A99. DOI: 10.1051/0004-6361/201118502. arXiv: 1111.5544 [astro-ph.HE].
- [22] E. Aliu et al. “Observation of Pulsed  $\gamma$ -Rays Above 25 GeV from the Crab Pulsar with MAGIC”. In: *Science* 322.5905 (Nov. 2008), p. 1221. DOI: 10.1126/science.1164718. arXiv: 0809.2998 [astro-ph].
- [23] Heinz Andernach and Fritz Zwicky. “English and Spanish Translation of Zwicky’s (1933) The Redshift of Extragalactic Nebulae”. In: *arXiv e-prints*, arXiv:1711.01693 (Nov. 2017), arXiv:1711.01693. arXiv: 1711.01693 [astro-ph.IM].
- [24] S. Archambault et al. “Dark matter constraints from a joint analysis of dwarf Spheroidal galaxy observations with VERITAS”. In: *Physical Review D* 95.8, 082001 (Apr. 2017), p. 082001. DOI: 10.1103/PhysRevD.95.082001. arXiv: 1703.04937 [astro-ph.HE].
- [25] Julia Becker Tjus et al. “Gamma-ray emitting supernova remnants as the origin of Galactic cosmic rays?” In: *Astroparticle Physics* 81 (Aug. 2016), pp. 1–11. DOI: 10.1016/j.astropartphys.2016.03.008. arXiv: 1510.07801 [astro-ph.HE].
- [26] Gianfranco Brunetti and Thomas W. Jones. “Cosmic Rays in Galaxy Clusters and Their Nonthermal Emission”. In: *International Journal of Modern Physics D* 23.4, 1430007–98 (Mar. 2014), pp. 1430007–98. DOI: 10.1142/S0218271814300079. arXiv: 1401.7519 [astro-ph.CO].
- [27] Matthew R. Buckley et al. “Search for gamma-ray emission from dark matter annihilation in the large magellanic cloud with the fermi large area telescope”. In: *Physical Review D* 91.10, 102001 (May 2015), p. 102001. DOI: 10.1103/PhysRevD.91.102001. arXiv: 1502.01020 [astro-ph.HE].
- [28] S. Chandrasekhar. “The Maximum Mass of Ideal White Dwarfs”. In: *Astrophysical Journal* 74 (July 1931), p. 81. DOI: 10.1086/143324.
- [29] Cherenkov Telescope Array Consortium et al. *Science with the Cherenkov Telescope Array*. 2019. DOI: 10.1142/10986.
- [30] Marco Cirelli et al. “Gamma ray constraints on decaying dark matter”. In: *Physical Review D* 86.8, 083506 (Oct. 2012), p. 083506. DOI: 10.1103/PhysRevD.86.083506. arXiv: 1205.5283 [astro-ph.CO].
- [31] *Classical Novae*. 2nd ed. Cambridge Astrophysics. Cambridge University Press, 2008. DOI: 10.1017/CBO9780511536168.
- [32] R. H. D. Corbet et al. “A Luminous Gamma-ray Binary in the Large Magellanic Cloud”. In: *Astrophysical Journal* 829.2, 105 (Oct. 2016), p. 105. DOI: 10.3847/0004-637X/829/2/105. arXiv: 1608.06647 [astro-ph.HE].

- [33] Bożena Czerny et al. “Astronomical Distance Determination in the Space Age. Secondary Distance Indicators”. In: *Space Science Reviews* 214.1, 32 (Feb. 2018), p. 32. DOI: 10.1007/s11214-018-0466-9. arXiv: 1801.00598 [astro-ph.GA].
- [34] Charles Dennison Dermer and Berrie Giebels. “Active galactic nuclei at gamma-ray energies”. In: *Comptes Rendus Physique* 17.6 (June 2016), pp. 594–616. DOI: 10.1016/j.crhy.2016.04.004. arXiv: 1602.06592 [astro-ph.HE].
- [35] A. Dominguez et al. “Extragalactic background light inferred from AEGIS galaxy-SED-type fractions”. In: *Monthly Notices of the RAS* 410.4 (Feb. 2011), pp. 2556–2578. DOI: 10.1111/j.1365-2966.2010.17631.x. arXiv: 1007.1459 [astro-ph.CO].
- [36] Guillaume Dubus. “Gamma-ray binaries and related systems”. In: *Astronomy and Astrophysics Reviews* 21, 64 (Aug. 2013), p. 64. DOI: 10.1007/s00159-013-0064-5. arXiv: 1307.7083 [astro-ph.HE].
- [37] Enrico Fermi. “On the Origin of the Cosmic Radiation”. In: Dec. 1972, pp. 238–252. ISBN: 9780080167244. DOI: 10.1016/B978-0-08-016724-4.50024-0.
- [38] Alberto Franceschini and Giulia Rodighiero. “The extragalactic background light revisited and the cosmic photon-photon opacity”. In: *Astronomy and Astrophysics* 603, A34 (July 2017), A34. DOI: 10.1051/0004-6361/201629684. arXiv: 1705.10256 [astro-ph.HE].
- [39] P. C. C. Freire et al. “Fermi Detection of a Luminous -Ray Pulsar in a Globular Cluster”. In: *Science* 334.6059 (2011), pp. 1107–1110. ISSN: 0036-8075. DOI: 10.1126/science.1207141. eprint: <https://science.sciencemag.org/content/334/6059/1107.full.pdf>. URL: <https://science.sciencemag.org/content/334/6059/1107>.
- [40] Bryan M. Gaensler and Patrick O. Slane. “The Evolution and Structure of Pulsar Wind Nebulae”. In: *Annual Review of Astron and Astrophys* 44.1 (Sept. 2006), pp. 17–47. DOI: 10.1146/annurev.astro.44.051905.092528. arXiv: astro-ph/0601081 [astro-ph].
- [41] Michael Gajdus. “The Vela pulsar in very high energy gamma-rays with H.E.S.S. II”. PhD thesis. Humboldt-Universität zu Berlin, Mathematisch-Naturwissenschaftliche Fakultät, 2016. DOI: <http://dx.doi.org/10.18452/17610>.
- [42] G. Ghirlanda et al. “Are short Gamma Ray Bursts similar to long ones?” In: *Journal of High Energy Astrophysics* 7 (2015). Swift 10 Years of Discovery, a novel approach to Time Domain Astronomy, pp. 81–89. ISSN: 2214-4048. DOI: <https://doi.org/10.1016/j.jheap.2015.04.002>. URL: <http://www.sciencedirect.com/science/article/pii/S2214404815000129>.
- [43] A. Goldwurm. “An Overview of the High-Energy Emission from the Galactic Center”. In: *The Galactic Center: a Window to the Nuclear Environment of Disk Galaxies*. Ed. by M. R. Morris, Q. D. Wang, and F. Yuan. Vol. 439. Astronomical Society of the Pacific Conference Series. May 2011, p. 391. arXiv: 1007.4174 [astro-ph.HE].
- [44] Andrea Goldwurm. “High energy activity of the super-massive black hole at the Galactic Center”. In: *Comptes Rendus Physique* 8 (Jan. 2007), pp. 35–44. DOI: 10.1016/j.crhy.2006.11.001. arXiv: 0705.4091 [astro-ph].

- [45] H. E. S. S. Collaboration et al. “Search for very-high-energy  $\gamma$ -ray emission from Galactic globular clusters with H.E.S.S.” In: *Astronomy and Astrophysics* 551, A26 (Mar. 2013), A26. DOI: 10.1051/0004-6361/201220719. arXiv: 1301.1678 [astro-ph.HE].
- [46] H. E. S. S. Collaboration et al. “The exceptionally powerful TeV  $\gamma$ -ray emitters in the Large Magellanic Cloud”. In: *Science* 347.6220 (Jan. 2015), pp. 406–412. DOI: 10.1126/science.1261313. arXiv: 1501.06578 [astro-ph.HE].
- [47] W. F. Hanlon. *Updated cosmic ray spectrum*. 2015. URL: <http://www.physics.utah.edu/~whanlon/spectrum.html>.
- [48] L. Hernquist. “An analytical model for spherical galaxies and bulges”. In: *Astrophysical Journal* 356 (June 1990), pp. 359–364. DOI: 10.1086/168845.
- [49] A. M. Hillas. “The Origin of Ultrahigh-Energy Cosmic Rays”. In: *Ann. Rev. Astron. Astrophys.* 22 (1984), pp. 425–444. DOI: 10.1146/annurev.aa.22.090184.002233.
- [50] Kouichi Hirotani. “High Energy Emission from Rotation-Powered Pulsars: Outer-gap vs. Slot-gap Models”. In: *arXiv e-prints*, arXiv:0809.1283 (Sept. 2008), arXiv:0809.1283. arXiv: 0809.1283 [astro-ph].
- [51] Xiaoyuan Huang, Gilles Vertongen, and Christoph Weniger. “Probing dark matter decay and annihilation with Fermi LAT observations of nearby galaxy clusters”. In: *Journal of Cosmology and Astroparticle Physics* 2012.1, 042 (Jan. 2012), p. 042. DOI: 10.1088/1475-7516/2012/01/042. arXiv: 1110.1529 [hep-ph].
- [52] Nu. Komin et al. “H.E.S.S. observations of the Large Magellanic Cloud”. In: *arXiv e-prints*, arXiv:1201.0639 (Jan. 2012), arXiv:1201.0639. arXiv: 1201.0639 [astro-ph.HE].
- [53] C. Kouveliotou et al. “Identification of two classes of gamma-ray bursts”. In: *Astrophysical Journal* 413 (Aug. 1993), pp. L101–L104. DOI: 10.1086/186969.
- [54] A. V. Kravtsov et al. “The Cores of Dark Matter-dominated Galaxies: Theory versus Observations”. In: *Astrophysical Journal* 502 (July 1998), pp. 48–58. DOI: 10.1086/305884. eprint: astro-ph/9708176.
- [55] M Kuhlen et al. “The Via Lactea INCITE simulation: galactic dark matter substructure at high resolution”. In: *Journal of Physics: Conference Series* 125 (July 2008), p. 012008. DOI: 10.1088/1742-6596/125/1/012008.
- [56] L. Kuiper et al. “The Crab pulsar in the 0.75–30 MeV range as seen by CGRO COMPTEL. A coherent high-energy picture from soft X-rays up to high-energy gamma-rays”. In: *Astronomy and Astrophysics* 378 (Nov. 2001), pp. 918–935. DOI: 10.1051/0004-6361:20011256. eprint: astro-ph/0109200.
- [57] Mariangela Lisanti. “Lectures on Dark Matter Physics”. In: *New Frontiers in Fields and Strings (TASI 2015)*. Jan. 2017, pp. 399–446. DOI: 10.1142/9789813149441\_0007. arXiv: 1603.03797 [hep-ph].
- [58] M. S. Longair. *High Energy Astrophysics*. 3rd ed. Cambridge University Press, 2011.
- [59] R. Mirzoyan. “First time detection of a GRB at sub-TeV energies; MAGIC detects the GRB 190114C”. In: *The Astronomer’s Telegram* 12390 (Jan. 2019).
- [60] J. F. Navarro, C. S. Frenk, and S. D. M. White. “The Structure of Cold Dark Matter Halos”. In: *Astrophysical Journal* 462 (May 1996), p. 563. DOI: 10.1086/177173. eprint: astro-ph/9508025.

- [61] Julio F. Navarro. “The Structure of Cold Dark Matter Halos”. In: *Symposium - International Astronomical Union* 171 (1996), pp. 255–258. DOI: 10.1017/S0074180900232452.
- [62] Stefan Ohm. “Starburst galaxies as seen by gamma-ray telescopes”. In: *Comptes Rendus Physique* 17.6 (June 2016), pp. 585–593. DOI: 10.1016/j.crhy.2016.04.003. arXiv: 1601.06386 [astro-ph.HE].
- [63] Keith A. Olive. “TASI Lectures on Dark Matter”. In: *arXiv e-prints*, astro-ph/0301505 (Jan. 2003), astro-ph/0301505. arXiv: astro-ph/0301505 [astro-ph].
- [64] D. E. Osterbrock and G. J. Ferland. *Astrophysics of gaseous nebulae and active galactic nuclei*. 2006.
- [65] Igor Oya Vallejo. “Observations of Active Galactic Nuclei with the MAGIC Telescope”. PhD thesis. UCM, Madrid, Dept. Phys., 2010. URL: <https://magiccold.mpp.mpg.de/publications/theses/I0ya.pdf>.
- [66] D. H. Perkins. *Particle Astrophysics*. 2nd ed. Oxford University Press, 2009.
- [67] T. Piran. “Gamma-ray bursts and the fireball model”. In: *Physics Reports* 314.6 (June 1999), pp. 575–667. DOI: 10.1016/S0370-1573(98)00127-6. arXiv: astro-ph/9810256 [astro-ph].
- [68] Tsvi Piran. “The physics of gamma-ray bursts”. In: *Reviews of Modern Physics* 76.4 (Oct. 2004), pp. 1143–1210. DOI: 10.1103/RevModPhys.76.1143. arXiv: astro-ph/0405503 [astro-ph].
- [69] Planck Collaboration et al. “Planck 2013 results. XVI. Cosmological parameters”. In: *Astronomy and Astrophysics* 571, A16 (Nov. 2014), A16. DOI: 10.1051/0004-6361/201321591. arXiv: 1303.5076 [astro-ph.CO].
- [70] Sara Rezaeikh et al. “The star formation history of the Magellanic Clouds derived from long-period variable star counts”. In: *Monthly Notices of the RAS* 445.3 (Dec. 2014), pp. 2214–2222. DOI: 10.1093/mnras/stu1807. arXiv: 1409.0790 [astro-ph.GA].
- [71] Thomas P. Robitaille and Barbara A. Whitney. “The Present-Day Star Formation Rate of the Milky Way Determined from Spitzer-Detected Young Stellar Objects”. In: *Astrophysical Journal* 710.1 (Feb. 2010), pp. L11–L15. DOI: 10.1088/2041-8205/710/1/L11. arXiv: 1001.3672 [astro-ph.GA].
- [72] V. C. Rubin, W. K. Ford Jr., and N. Thonnard. “Extended rotation curves of high-luminosity spiral galaxies. IV - Systematic dynamical properties, SA through SC”. In: *Astrophysical Journal* 225 (Nov. 1978), pp. L107–L111. DOI: 10.1086/182804.
- [73] M. A. Ruderman and P. G. Sutherland. “Theory of pulsars - Polar caps, sparks, and coherent microwave radiation”. In: *Astrophysical Journal* 196 (Feb. 1975), pp. 51–72. DOI: 10.1086/153393.
- [74] V. Schönfelder. *The Universe in Gamma Rays*. 2001, p. 407.
- [75] Joshua D. Simon and Marla Geha. “The Kinematics of the Ultra-faint Milky Way Satellites: Solving the Missing Satellite Problem”. In: *Astrophysical Journal* 670.1 (Nov. 2007), pp. 313–331. DOI: 10.1086/521816. arXiv: 0706.0516 [astro-ph].
- [76] Julian Sitarek and Włodek Bednarek. “GeV-TeV gamma rays and neutrinos from the Nova V407 Cygni”. In: *Physical Review D* 86.6, 063011 (Sept. 2012), p. 063011. DOI: 10.1103/PhysRevD.86.063011. arXiv: 1208.6200 [astro-ph.HE].

- [77] Yoshiaki Sofue. “Dark Bulge, Exponential Disk, and Massive Halo in the Large Magellanic Cloud”. In: *Publications of the Astronomical Society of Japan* 51.4 (Aug. 1999), pp. 445–448. ISSN: 0004-6264. DOI: 10.1093/pasj/51.4.445. eprint: <http://oup.prod.sis.lan/pasj/article-pdf/51/4/445/9716974/pasj51-0445.pdf>. URL: <https://doi.org/10.1093/pasj/51.4.445>.
- [78] P. Sreekumar et al. “Observations of the Large Magellanic Cloud in High-Energy Gamma Rays”. In: *Astrophysical Journal* 400 (Dec. 1992), p. L67. DOI: 10.1086/186651.
- [79] Meng Su, Tracy R. Slatyer, and Douglas P. Finkbeiner. “Giant Gamma-ray Bubbles from Fermi-LAT: Active Galactic Nucleus Activity or Bipolar Galactic Wind?” In: *Astrophysical Journal* 724.2 (Dec. 2010), pp. 1044–1082. DOI: 10.1088/0004-637X/724/2/1044. arXiv: 1005.5480 [astro-ph.HE].
- [80] Pak-Hin T. Tam, Chung Y. Hui, and Albert K. H. Kong. “Gamma-ray Emission from Globular Clusters”. In: *Journal of Astronomy and Space Sciences* 33.1 (Mar. 2016), pp. 1–11. DOI: 10.5140/JASS.2016.33.1.1. arXiv: 1207.7267 [astro-ph.HE].
- [81] C. Megan Urry and Paolo Padovani. “Unified Schemes for Radio-Loud Active Galactic Nuclei”. In: *Publications of the Astronomical Society of the Pacific* 107 (Sept. 1995), p. 803. DOI: 10.1086/133630. arXiv: astro-ph/9506063 [astro-ph].
- [82] Roeland P. van der Marel. “The Large Magellanic Cloud: structure and kinematics”. In: *The Local Group as an Astrophysical Laboratory*. Ed. by Mario Livio and Thomas M. Brown. Vol. 17. Jan. 2006, pp. 47–71. arXiv: astro-ph/0404192 [astro-ph].
- [83] VERITAS Collaboration et al. “A connection between star formation activity and cosmic rays in the starburst galaxy M82”. In: *Nature* 462.7274 (Dec. 2009), pp. 770–772. DOI: 10.1038/nature08557. arXiv: 0911.0873 [astro-ph.CO].
- [84] S. P. Wakely and D. Horan. “TeVCat: An online catalog for Very High Energy Gamma-Ray Astronomy”. In: *International Cosmic Ray Conference* 3 (2008), pp. 1341–1344.
- [85] Kurt W. Weiler and Richard A. Sramek. “Supernovae and supernova remnants.” In: *Annual Review of Astron and Astrophys* 26 (Jan. 1988), pp. 295–341. DOI: 10.1146/annurev.aa.26.090188.001455.
- [86] J. H. K. Wu et al. “SEARCH FOR PULSED  $\gamma$ -RAY EMISSION FROM GLOBULAR CLUSTER M28”. In: *The Astrophysical Journal* 765.2 (Feb. 2013), p. L47. DOI: 10.1088/2041-8205/765/2/147.
- [87] Shao-Qiang Xi et al. “Detection of gamma-ray emission from the Coma cluster with Fermi Large Area Telescope and tentative evidence for an extended spatial structure”. In: *Physical Review D* 98.6, 063006 (Sept. 2018), p. 063006. DOI: 10.1103/PhysRevD.98.063006. arXiv: 1709.08319 [astro-ph.HE].
- [88] H. Zhao. “Analytical models for galactic nuclei”. In: *Monthly Notices of the RAS* 278 (Jan. 1996), pp. 488–496. DOI: 10.1093/mnras/278.2.488. eprint: astro-ph/9509122.





## Acronyms

**AGN** Active Galaxy Nuclei. 4, 5, 10, 11, 20, 22, 23

**BH** Black Hole. 23, 24

**CDM** Cold Dark Matter. 15, 27

**CMB** Cosmic Microwave Background. 10, 12, 15, 25

**COMPTEL** Imaging Compton Telescope. 18

**CR** Cosmic Ray. 4, 5, 7, 8, 19, 24–26

**DM** Dark Matter. 13, 15–17, 25–29

**DSA** Diffusive Shock Acceleration. 5, 7

**DSphe** Dwarf Spheroidal Galaxies. 27

**EAS** Extended Air Showers. 12

**EBL** Extragalactic Background Light. 12, 13, 23

**EGRET** Energetic Gamma Ray Experiment Telescope. 18, 26

**GC** Galactic Center. 21, 22, 26

**GRB** Gamma Ray Burst. 4, 5, 23–25

**H.E.S.S.** High Energy Stereoscopic System. 17, 21, 22, 26, 29

**HE** High Energy. 10, 12, 20–22, 24–26, 29

**ic** Inverse Compton. 10, 20–22, 25

**ICM** Intracluster Medium. 25

**ISM** Interstellar Medium. 4, 5, 7, 12, 19, 24–26

**LMC** Large Magellanic Cloud. 26, 29

**MAGIC** Major Atmospheric Gamma Imaging Cherenkov Telescopes. 17, 18, 21, 24, 29

**MSP** Millisecond Pulsar. 22

**PWN** Pulsar Wind Nebula. 3, 19, 20

**PWNe** Pulsar Wind Nebulae. 19–21

**SFR** Star Formation Rate. 24

**SM** Standard Model. 15, 16

**SMBH** Super Massive Black Hole. 21, 23

**SMC** Small Magellanic Cloud. 26

**SN** Supernova. 5, 7, 19, 20, 22, 24

**SNR** Supernova Remnant. 4, 5, 8, 11, 19–21, 24–26

**SUSY** Super Symmetry. 16

**UHECR** Ultra High Energy Cosmic Ray. 10

**VERITAS** Very Energetic Radiation Imaging Telescope Array System. 17

**VHE** Very High Energy. 3, 10, 12, 13, 17, 18, 20, 23–26, 29

**WIMP** Weak Interacting Massive Particle. 16, 26

**WMAP** Wilkinson Microwave Anisotropy Probe. 15, 16, 22